

1 **Geminiviruses Subvert Ubiquitination by Altering CSN-Mediated Derubylation of SCF E3**
2 **Ligase Complexes and Inhibit Jasmonate Signaling in Arabidopsis thaliana**~~The C4 protein~~
3 ~~from the geminivirus Tomato yellow leaf curl virus confers drought tolerance in~~
4 ~~Arabidopsis through an ABA-independent mechanism~~

5
6 Rosa Lozano-Durán¹, Tabata Rosas-Díaz¹, Giuliana Gusmaroli², Ana P. Luna¹, Ludivine
7 Tacconat³, Xing Wang Deng², Eduardo R. Bejarano¹

8 ¹Instituto de Hortofruticultura Subtropical y Mediterránea “La Mayora” (IHSM-UMA-CSIC),
9 Departamento de Genética, Facultad de Ciencias, Universidad de Málaga, Campus de Teatinos
10 s/n, E-29071 Málaga, Spain; ²Department of Molecular, Cellular, and Developmental Biology,
11 Yale University, New Haven, Connecticut 06520-8104; ³. Unité Mixte de Recherche, Institut
12 National de la Recherche Agronomique 1165, Centre National de la Recherche Scientifique 8114,
13 UEVE, 91057 Evry, France

14 Corresponding author: E. R. Bejarano; E-mail: Edu_rodri@uma.es¹~~Shanghai Center for Plant~~
15 ~~Stress Biology, Chinese Academy of Sciences, Shanghai 201602, China; Center for Excellence~~
16 ~~in Molecular Plant Science, Chinese Academy of Sciences.~~²~~Instituto de Hortofruticultura~~
17 ~~Subtropical y Mediterránea “La Mayora” (IHSM-UMA-CSIC), Area~~~~Área de Genética, Facultad de~~
18 ~~Ciencias, Universidad de Málaga, Campus de Teatinos s/n, E-29071 Málaga, Spain.~~³~~University~~
19 ~~of the Chinese Academy of Sciences, Beijing 100049, China~~

20 **ABSTRACT:**

21 Viruses must create a suitable cell environment and elude defense mechanisms, which likely
22 involves interactions with host proteins and subsequent interference with or usurpation of cellular
23 machinery. Here, we describe a novel strategy used by plant DNA viruses (Geminiviruses) to
24 redirect ubiquitination by interfering with the activity of the CSN (COP9 signalosome) complex.
25 We show that geminiviral C2 protein interacts with CSN5, and its expression in transgenic plants
26 compromises CSN activity on CUL1. Several responses regulated by the CUL1-based SCF
27 ubiquitin E3 ligases (including responses to jasmonates, auxins, gibberellins, ethylene, and
28 abscisic acid) are altered in these plants. Impairment of SCF function is confirmed by stabilization
29 of yellow fluorescent protein–GAI, a substrate of the SCF^{SLY1}. Transcriptomic analysis of these
30 transgenic plants highlights the response to jasmonates as the main SCF-dependent process
31 affected by C2. Exogenous jasmonate treatment of Arabidopsis thaliana plants disrupts

32 geminivirus infection, suggesting that the suppression of the jasmonate response might be crucial
33 for infection. Our findings suggest that C2 affects the activity of SCFs, most likely through
34 interference with the CSN. As SCFs are key regulators of many cellular processes, the capability
35 of viruses to selectively interfere with or hijack the activity of these complexes might define a novel
36 and powerful strategy in viral infections..

37 **INTRODUCTION:**

38 Members of the Geminivirus family are plant viruses with circular, single-stranded DNA genomes
39 (Rojas et al., 2005) that infect a wide range of plant species and cause extensive losses in food
40 and fiber crops. Geminiviruses have highly reduced genomes, encoding only six to eight proteins.
41 Due to limiting coding capacity, to successfully accomplish infection, these viruses must rely on
42 both their own multifunctional proteins and the host cell machinery to replicate, move within and
43 between cells, and avoid plant defense mechanisms (Hanley-Bowdoin et al., 2004).

44

45 C2 (also known as L2, AC2, AL2, or TrAP, for transcriptional activator protein) is a multifunctional
46 protein encoded by geminiviruses. In viruses belonging to the genus Begomovirus, C2 acts as a
47 transcription factor required for the expression of viral genes needed late in infection (Sunter and
48 Bisaro, 1992) and triggers transactivation of host genes (Trinks et al., 2005) through an indirect
49 mechanism. C2 is also a pathogenicity factor that suppresses host defenses: constitutive
50 expression of truncated C2 from the begomovirus Tomato golden mosaic virus or the related L2
51 protein from the curtovirus Beet curly top virus (BCTV) in transgenic plants conditions an
52 enhanced susceptibility phenotype (Sunter et al., 2001) that correlates with their ability to interact
53 with and inactivate SNF1-related kinase (Sunter et al., 2001; Hao et al., 2003). C2 and L2 are
54 also gene silencing suppressors of both posttranscriptional gene silencing and transcriptional
55 gene silencing (reviewed in Raja et al., 2010).

56

57 Plants are sessile organisms forced to face environmental variations and continuously challenged
58 by potential pathogens. To mount a rapid response, plants extensively rely on proteomic plasticity,
59 which is partially driven by ubiquitination, a highly dynamic posttranslational modification that
60 controls most of the protein degradation events in eukaryotes. According to proteomic and genetic
61 analyses, ubiquitination rivals transcription as the dominant regulatory mechanism in plants
62 (Vierstra, 2009). Ubiquitination occurs through an enzymatic cascade comprising an E1 ubiquitin

63 activating enzyme, an E2 ubiquitin conjugating enzyme, and an E3 ubiquitin ligase that binds the
64 substrate and thus confers specificity. In plants, the most abundant family of E3 ligases comprises
65 the multisubunit Cullin RING Ligases (CRLs). Among these, the Cullin1-based group, also named
66 SCF (for Skp1/Cullin1/F-box), is the largest and best characterized because of its unveiled roles
67 in many cellular processes, such as hormonal responses (reviewed in Dreher and Callis, 2007;
68 Santner and Estelle, 2009), light signaling (Dieterle et al., 2001; Harmon and Kay, 2003; Marrocco
69 et al., 2006), or floral meristem and organ identity (Kuroda et al., 2002; Wang et al., 2003). SCF
70 complexes are composed of four subunits: Cullin1 (CUL1), SKP1/ASK (S-phase kinase-
71 associated protein), the RING subunit RBX1 (RING box 1), and an F-box substrate binding protein.
72 The *Arabidopsis thaliana* genome encodes more than 700 predicted F-box proteins, which
73 suggests a high targeting potential (Hua et al., 2011).

74

75 The activity of Cullin RING ligases is regulated by a cycle of covalent attachment and removal of
76 a ubiquitin-like protein named RUB (for Related to Ubiquitin; known as Nedd8 in fission yeast and
77 animals) (del Pozo and Estelle, 1999; reviewed in Hotton and Callis, 2008), which is needed for
78 robust CRL activity (Lyapina et al., 2001). One of the regulators of this activity is a conserved
79 protein complex named CSN (COP9 signalosome; reviewed in Wei et al., 2008). The CSN
80 complex is comprised of eight subunits, named CSN1 to CSN8, where CSN5 is the only catalytic
81 subunit described to date. The best-characterized biochemical activity assigned to the CSN is the
82 isopeptidase activity that removes the RUB moiety from the cullin component of the CRL, which
83 is essential for the function of CRLs in vivo. In addition to the CSN holocomplex, several other
84 subcomplexes are formed by a subset of CSN subunits or by CSN5 and other proteins, but the
85 composition and number of these small complexes still remain unclear (Mundt et al., 2002; Oron
86 et al., 2002; Gusmaroli et al., 2004; Fukumoto et al., 2005; Tomoda et al., 2005). Ubiquitination
87 has been shown to contribute to multiple levels of plant defense (reviewed in Dreher and Callis,
88 2007). Specifically, several lines of evidence suggest that SCF complexes function in plant-virus
89 interactions: (1) SGT1, an essential SKP1-interacting eukaryotic protein, is required for host and
90 nonhost resistance, virus-induced necrosis, and restraint of viral growth of *Plantago asiatica*
91 mosaic virus and Potato virus X (Komatsu et al., 2010); (2) virus-induced gene silencing of SKP1,
92 SGT1, or the CSN complex compromised N gene-mediated resistance to Tobacco mosaic virus
93 (TMV) in *Nicotiana benthamiana* (Liu et al., 2002); (3) the F-box protein ACIF is needed for TMV-
94 triggered hypersensitive response in *Nicotiana tabacum* and affects N gene-mediated responses
95 to TMV (van den Burg et al., 2008).

96

97 A large number of both animal and plant viruses have been described to interfere, inhibit, or usurp
98 the ubiquitination machinery in the cell (reviewed in Isaacson and Ploegh, 2009) by encoding their
99 own ubiquitination components (ubiquitin-like proteins, E3 ligases, adaptors, or deubiquitinating
100 enzymes) or redirecting host ubiquitination. In plants, the Ploverovirus P0 protein carries an F-box
101 domain that allows its incorporation into an SCF complex to mediate degradation of AGO1,
102 modulating gene silencing (Baumberger et al., 2007; Bortolamiol et al., 2007). The nanovirus Clink
103 protein is also an F-box protein and can bind to both SKP1 and the cell cycle protein pRBR,
104 affecting cell cycle regulation (Aronson et al., 2000).

105

106 Ubiquitination controls most of the hormonal responses in plants (reviewed in Dreher and Callis,
107 2007; Santner and Estelle, 2009). Among them, the jasmonate response, dependent on the
108 SCFCO11 complex, plays a crucial role in pathogen defenses. Not much information about the
109 role of jasmonates on viral infection is currently available, but recent works revealed jasmonate
110 signaling as an emerging topic in plant–virus interaction research (Vigliocco et al., 2002; Liu et al.,
111 2004; Agudelo-Romero et al., 2008; Ascencio-Ibáñez et al., 2008; Yang et al., 2008; Kovac et al.,
112 2009).

113

114 In this article, we demonstrate that geminiviruses, through their C2 protein, interact and interfere
115 with the derubylation activity of the CSN complex. The activity of the CSN over CUL1 seems to
116 be compromised when C2 is present; consequently, processes regulated by SCF complexes are
117 altered. Since SCFs are key regulators of many cellular processes, the capability of geminiviruses
118 to selectively interfere with or hijack the activity of these complexes might represent a powerful
119 strategy in the viral infection. According to our results, one of the main targets of geminiviral
120 inhibition of SCFs might be the suppression of the jasmonate response. This work demonstrates
121 that geminiviruses are capable of interfering with the ubiquitination pathway and jasmonate
122 signaling through a novel mechanism.

123 **RESULTS**

124 **TYLCSV C2 Is Required for Full Infection.**

125 Several geminiviral proteins are required to accomplish full infection. Among them, C2 from
126 several begomoviruses has been shown to be needed for viral propagation (Etessami et al., 1988;

127 Wartig et al., 1997). To confirm if this is also applicable to Tomato yellow leaf curl Sardinia virus
128 Spain isolate (TYLCSV; accession number L27708), one of the begomoviruses responsible for
129 the Tomato yellow leaf curl disease (TYLCD) in Spain, we constructed a null mutant virus for the
130 C2 gene with a T-C transition in the start codon, hereafter called TYLCSV C2T2C. This mutation
131 also affects the nucleotide sequence of Rep (for Replication-associated protein) viral gene but
132 does not result in an amino acid change. TYLCSV C2T2C was unable to infect tomato, while *N.*
133 *benthamiana* plants infected with the mutant developed very mild or no symptoms and the level
134 of viral DNA was severely reduced (see Supplemental Figure 1A online). To confirm that the viral
135 DNA accumulated in plants infected with the mutant does not result from replication of revertants,
136 we extracted DNA from young leaves collected at 28 d after inoculation (DAI) from plants
137 inoculated with the mutant virus (three infected plants). A 625-bp fragment containing the mutation
138 site was PCR amplified and fully sequenced. All analyzed fragments contained the mutation,
139 confirming that the T-C transition is stable in infected plants.

140

141 To determine if the mutant is affected in replication, we evaluated the level of viral DNA
142 accumulated in agroinfiltrated leaf patches of *N. benthamiana*. Total DNA was extracted 7 d after
143 infiltration and hybridized with a TYLCSV probe. TYLCSV C2T2C DNA accumulates to levels
144 comparable to those of the wild-type virus, indicating that the mutant is not impaired in replication
145 (see Supplemental Figure 1B online). These results indicate that C2 from the Spanish isolate of
146 TYLCSV is required for the establishment of a systemic infection but not for viral replication.

147 **C2 Interacts with the Plant CSN5.**

148 Protein–protein interactions between viral and host proteins are one of the main mechanisms
149 used by viruses to create a proper environment for the infection. To identify plant proteins
150 interacting with C2, we performed a wide yeast two-hybrid screen using an *Arabidopsis* cDNA
151 library (F. Hericourt, C. Grevesse, D. Colinet, S. Déret, E.R. Bejarano, and A. Khashoggi,
152 unpublished data). For the screening, a partial clone of C2, named C2-TS1-78, lacking 59 amino
153 acids of the C terminus, was expressed fused to GAL4 DBD. This truncated C2 protein lacks the
154 transcriptional activation domain, since this domain has been previously shown to activate the
155 expression of yeast two-hybrid GAL4 system reporter genes by itself (Hartitz et al., 1999). One of
156 five clones identified in the screening (from 2×10^7 transformants) corresponds to a truncated
157 version of the *Arabidopsis* CSN5A lacking the 44 N-terminal amino acids (CSN5A44-357).

158

159 CSN5A is the only catalytic subunit of the conserved eukaryotic multiprotein complex named CSN
160 described to date. CSN, originally identified through genetic screening as a negative regulator of
161 photomorphogenesis in Arabidopsis, has been subsequently involved in the regulation of a wide
162 variety of signaling and developmental processes in multiple organisms across all eukaryotic
163 kingdoms, and its activity has proven to be essential. In Arabidopsis, transgenic lines expressing
164 dominant-negative versions of CSN5A (Gusmaroli et al., 2004) or mutants partially defective in
165 CSN5 activity (Gusmaroli et al., 2007) display severe pleiotropic developmental defects. On the
166 other hand, complete loss of function of any of the eight CSN subunits results in a lethal phenotype
167 characterized by postembryonic arrest at seedling stage (Gusmaroli et al., 2007). Despite its
168 involvement in the regulation of a plethora of developmental and environmental responses, the
169 major biochemical activity ascribed to date to the CSN is the removal of RUB1 from cullins.

170

171 To analyze if the interaction between C2 and CSN5 is conserved throughout the geminivirus
172 family, we assayed the interaction of Arabidopsis CSN5A with C2 homologs from two other
173 geminivirus species: C2 from the begomovirus Tomato yellow leaf curl virus (TYLCV), another
174 causal agent of TYLCD, and L2 from the curtovirus BCTV, which is able to infect Arabidopsis.
175 Hereafter, C2-TS stands for TYLCSV C2, C2-TM stands for TYLCV C2, and L2-BC stands for
176 BCTV L2. Although C2 and L2 share similar roles, since both inhibit RNA silencing and act as
177 pathogenicity factors, they show some functional divergence: C2 also functions as a transcription
178 factor, while apparently L2 does not. Like for TYLCSV C2, partial clones encoding C-terminal
179 truncated TYLCV C2 or BCTV L2, named C2-TM1-78 and L2-BC1-108, respectively, were used
180 for the yeast two-hybrid assays. The C2 protein of both geminivirus species was shown to interact
181 with CSN5A44-357 in a yeast two-hybrid assay (Table 1), indicating that this interaction is
182 conserved among geminiviruses.

183 Phylogenetic analysis shows that CSN5 is highly conserved among plants (see Supplemental
184 Figure 2 online). In Arabidopsis, unlike any other plant species described so far, there are two
185 different CSN5 subunits, named CSN5A and CSN5B. These subunits display very different
186 abundance and incorporate into distinct CSN complexes (CSNCSN5A and CSNCSN5B) that play
187 unequal roles in the regulation of plant development (Gusmaroli et al., 2004).

188

189 To determine if C2 also interacts with CSN5B, we cloned a partial CSN5B clone, equivalent to
190 the CSN5A partial clone isolated in the screening, lacking the 44 N-terminal residues (CSN5B44-

191 358), and found that all three tested C2/L2 proteins are able to interact with Arabidopsis
192 CSN5B44-358 (Table 1). Given that TYLCSV and TYLCV are important pathogens for tomato
193 (*Solanum lycopersicum*) crops and tomato is a host for BCTV, we also tested the interaction
194 between C2/L2 and tomato CSN5. We cloned the CSN5 cDNA from *S. lycopersicum* cultivar
195 Moneymaker (AC:FN820438) and generated a partial clone to express a truncated protein similar
196 to the Arabidopsis CSN5A and CSN5B used in the binding assays (residues 57 to 367,
197 SICSN557-367). There are three amino acid differences between the cloned CSN5, obtained from
198 Moneymaker, and a previously identified CSN5 obtained from the VFNT cultivar (AC:AF175964).
199 Yeast two-hybrid assays demonstrate that all three tested C2 proteins are also able to interact
200 with SICSN557-367 (Table 1), suggesting that C2/L2-CSN5 interaction is also conserved in other
201 plant species.

202

203 It has been previously reported that CSN5 interacts with the GAL4 DNA binding domain (Nordgård
204 et al., 2001); thus, the isolation of CSN5 in a GAL4-based yeast two-hybrid screening should be
205 considered cautiously. However, CSN5 homologs from different organisms have been isolated in
206 this kind of screening in several independent studies (Kameda et al., 2006; Cho et al., 2008;
207 Tanguy et al., 2008), and the interactions have been confirmed by other methods. Curiously, in
208 two out of the three cited works, the isolated clone was partial, lacking at least the 44 N-terminal
209 amino acids. We found that the complete CSN5 proteins from both Arabidopsis (CSN5A and
210 CSN5B) and tomato, fused to the GAL4 AD, strongly interact with any protein fused to the GAL4
211 DBD or with the empty GAL4 DBD-containing vector. However, this unspecific interaction does
212 not occur when the truncated version of CSN5 is used instead.

213

214 To confirm the C2/L2-CSN5 interaction in planta, we used a bimolecular fluorescence
215 complementation (BiFC) assay. *N. benthamiana* leaves were coinfiltrated with *Agrobacterium*
216 *tumefaciens* cells to express N-terminal fusions of C2 or L2 with N- or C-yellow fluorescent protein
217 (YFP) and N-terminal fusions of Arabidopsis CSN5A or tomato CSN5 with C- or N-YFP. The
218 infiltrated leaves were analyzed under the confocal microscope 3 d after infiltration. YFP
219 fluorescence was observed in cells coinfiltrated with constructs corresponding to NYFP-CSN5A
220 and any of the CYFP-C2/L2 constructs or vice versa. Similar results were obtained when leaves
221 were coinfiltrated with tomato CSN5 and C2 constructs (Figure 1A). By contrast, expression of
222 CSN5 or any of C2/L2 constructs alone (data not shown) or coexpression of any of those

223 constructs with the β -glucuronidase protein (Kertbundit et al., 1991) fused to NYFP or CYFP did
224 not restore the YFP fluorescence (Figure 1). Interactions between C2/L2 and CSN5 seem to occur
225 mainly in the nuclei, as they colocalize with 4',6-diamidino-2-phenylindole (DAPI) staining (Figure
226 1A). The nuclear localization of C2 from some begomoviruses has been previously reported (van
227 Wezel et al., 2001; Sharma et al., 2010). To confirm that this is also the case for C2-TS,
228 subcellular localization was examined using a green fluorescent protein (GFP)-C2-TS fusion.
229 Three days after agroinfiltration of the construct in *N. benthamiana* leaves, agroinfiltrated patches
230 were observed under the confocal microscope. GFP-C2-TS localized mainly in the nucleus, as
231 demonstrated by the colocalization with DAPI staining (Figure 1B).

232 Taken together, these results demonstrate that C2/L2 from TYLCSV, TYLCV, and BCTV
233 associate with CSN5 mainly in the nucleus of plant cells.

234 **Expression of Viral C2/L2 Protein in Transgenic Arabidopsis Lines Specifically Interferes**
235 **with CUL1 Derubylation without Affecting the Proper Assembly of CSN and SCF**
236 **Complexes.**

237 To determine if the interaction of C2/L2 with CSN5 might be affecting the derubylation activity of
238 the CSN complex, we compared the relative levels of rubylated and derubylated cullins between
239 the wild-type and transgenic Arabidopsis plants expressing C2/L2 from TYLCSV, TYLCV, and
240 BCTV (details of these transgenic lines are shown in Supplemental Figure 3 online). None of
241 these C2/L2-expressing transgenic lines displayed noticeable defects in development or
242 morphology. Protein extracts from wild-type, transgenic C2/L2 lines and the *csn5a-1* mutant (as
243 a control) were subjected to immunoblot analysis using antibodies against Arabidopsis CUL1,
244 CUL3, and CUL4, the three Arabidopsis cullins known to form CRLs. As shown in Figure 2A, the
245 relative level of rubylated CUL1 observed in all transgenic lines expressing C2/L2 is higher than
246 that of the wild-type plants, whereas we did not observe clear changes in the relative rubylation
247 levels of CUL3 or CUL4 (see Supplemental Figure 4 online). This result suggests that C2/L2 may
248 be hindering the derubylating activity of the CSN complex specifically over CUL1. It is noteworthy
249 that the total cellular levels of CUL3 and CUL1 are slightly increased in the C2/L2 transgenic
250 plants; however, no changes in CUL4 accumulation are detected.

251 Viral proteins have often been shown to sequester host proteins to co-opt or redirect pivotal
252 cellular machineries to viral function. In this context, it is possible to speculate that C2/L2 might
253 sequester CSN5, preventing its assembly into the complex, or that C2/L2-CSN5 interaction might
254 affect the distribution of CSN5 between the CSN holocomplex and the CSN5-containing

255 subcomplex forms. Based on this idea, a gel filtration experiment was performed in which the
256 fractionation pattern of CSN5 was analyzed (Figure 2B). The comparison of the gel filtration
257 profiles of wild-type plants and transgenic lines expressing C2/L2 demonstrates that CSN5 is
258 normally assembled into both the CSN holocomplex, where it exercises its derubylation activity,
259 and into the subcomplex forms. Keeping in mind that the expression of C2/L2 results in the
260 accumulation of preferentially rubylated CUL1, it is also possible that these viral proteins could
261 alter CUL1 assembly into the SCF complex. However, the analyses of CUL1 fractionation patterns
262 did not reveal any significant changes in the presence of C2/L2 (Figure 2C). These results imply
263 that C2/L2 does not interfere with the proper assembly of CUL1 into the SCF complex. This is in
264 agreement with the observation that RBX1 and SKP1, two other components of the SCF complex,
265 accumulate in the same fractions in one representative C2 transgenic line (Figure 2D). Taken
266 together, these data indicate that C2/L2 does not interfere with the assembly of either the CSN or
267 the SCF complexes and that the observed accumulation of rubylated CUL1 is therefore consistent
268 with a specific interference of C2/L2 with the CSN-mediated CUL1 derubylation.

269 **C2/L2 Arabidopsis Transgenic Plants Share Phenotypes with cul1 Mutants, Including**
270 **Altered SCF-Dependent Hormonal Responses.**

271 Given that C2/L2 transgenic plants display an altered CUL1 rubylated/derubylated ratio, CUL1
272 function could be impaired in these plants. cul1 mutants are altered in a plethora of developmental
273 processes, such as root growth, skotomorphogenesis, and hormonal responses (Moon et al.,
274 2007; Gilkerson et al., 2009); consequently, it is conceivable that the C2/L2 transgenic plants
275 could also display these defects.

276 To evaluate root growth rate in the C2/L2 transgenic plants, the root length of 4-d-old seedlings
277 was measured every 24 h for 4 d. Data show that C2/L2 transgenic roots are smaller and grow
278 more slowly than wild-type roots (Figure 3A).

279 Skotomorphogenesis is also altered in transgenic C2/L2 plants: etiolated transgenic seedlings
280 differ from the wild type in hypocotyl length. All three transgenic lines display significantly shorter
281 hypocotyls than the wild type as determined by Mann-Whitney rank sum test (Figure 3B). The
282 reduction in hypocotyl size correlates with the RNA expression level of the transgenes (see
283 Supplemental Figure 5 online).

284 Because SCF complexes play a role in the signaling pathways of several hormones, and most of
285 these responses have been shown to be altered in cul1 mutants (Moon et al., 2007; Gilkerson et
286 al., 2009), we investigated how C2/L2 transgenic lines respond to ethylene, auxins, gibberellins,

287 and jasmonates. In all cases, we measured inhibition of primary root elongation caused by
288 treatment with the exogenous compound (1-aminocyclopropane-1-carboxylic acid [ACC], 2,4-D,
289 gibberellin A3 [GA3], or methyl jasmonate [MeJA]) as a measure of the response to the hormone.
290 The results show that Arabidopsis transgenic plants expressing C2 or L2 were less sensitive to
291 2,4-D, GA3, and MeJA and more sensitive to ACC (Figure 4). The differential sensitivity of C2/L2
292 transgenic plants is thus consistent with a malfunction of the corresponding SCF complex in all
293 cases. We tested the differential sensitivity to MeJA in independent transgenic lines expressing
294 different levels of C2/L2 mRNA and found a correlation between lower sensitivity and higher
295 mRNA expression (see Supplemental Figure 6A online). To confirm these results, quantitative
296 real-time PCR was used to quantify the mRNA expression level of marker genes for each of the
297 assayed hormones. We selected ERF1 and ERS1 as marker genes for the ethylene response,
298 PIN1 and IAA19 for the auxin response, MFC19.13 and MHJ24.10 for the gibberellin response,
299 and OPR3 and JR1 for the jasmonate response. In all cases, the expression level of the marker
300 genes correlated with the observed differential sensitivity phenotype (Figure 5). We also tested if
301 the expression of C2-TS alters the sensitivity to hormones in a different plant species: transgenic
302 *N. benthamiana* plants containing a TYLCSV C2 expression cassette were tested for their
303 sensitivity to auxins and jasmonates. As shown in Supplemental Figure 6B online, transgenic *N.*
304 *benthamiana* plants expressing C2-TS are also less sensitive to 2,4-D and MeJA, which
305 demonstrates that C2-mediated lower sensitivity to these hormones is not host specific.

306 Besides the previously described phenotypes, Arabidopsis C2/L2 transgenic plants are more
307 resistant to drought (Figure 6A). This enhanced tolerance correlated with a slower weight loss in
308 detached leaves (Figure 6B), suggesting that the stomata are more efficiently closed in these
309 plants. Recently, an F-box protein named DOR was described to function as an inhibitor for
310 abscisic acid (ABA)-induced stomatal closure under drought stress, most probably through its
311 activity in a SCFDOR complex (Zhang et al., 2008). The DOR gene is preferentially expressed in
312 the guard cells and affects the stomatal response to ABA: guard cells of the *dor* mutant are
313 hypersensitive to this hormone. However, other well-characterized responses to ABA, such as
314 the inhibition of seed germination or the reduction of vegetative growth, are not altered in this
315 mutant (Zhang et al., 2008), consistently with the specific expression pattern. Based on our
316 previous findings that C2/L2 seems to be interfering with the SCF complexes, it would be feasible
317 to speculate that a defective SCFDOR activity could result in increased ABA sensitivity in the
318 guard cells, which would in turn explain the observed drought tolerance phenotype. In line with
319 this idea, when we tested the stomatal response to exogenously applied ABA, we found that the
320 stomata in the C2/L2 transgenic plants are indeed more responsive to ABA (Figures 6C and 6D),

321 even though the sensitivity to this hormone is not higher when measured as inhibition of either
322 seed germination or root growth.

323 **C2/L2 Hinders the Degradation of GAI, Target of the SCFSLY1 E3.**

324 If the differential sensitivity to hormones observed in the C2/L2-expressing lines is due to the
325 inhibition of the SCF complexes, the substrates of these complexes must be accumulating in the
326 presence of C2/L2. To check this possibility, we took advantage of a YFP-GAI expression
327 construct (kindly provided by David Alabadí, Instituto de Biología Molecular y Celular de Plantas,
328 Spain). GAI is a DELLA protein that is degraded by the SCFSLY1 in the presence of gibberellins.
329 When the construct expressing YFP-GAI is agroinfiltrated in *N. benthamiana* leaves, yellow
330 fluorescence can be observed in the nuclei 3 DAI (Figure 7A), indicating the expression and
331 accumulation of the fusion protein. This fluorescence diminishes and eventually disappears when
332 the leaves are treated with 100 μ M GA3, since the hormone treatment triggers the ubiquitination
333 of the fusion protein by the SCFSLY1 and its subsequent degradation by the 26S proteasome.
334 As shown in Figure 7A, when we coinfiltrate YFP-GAI and C2/L2 expression construct, the
335 decrease in fluorescence after GA3 treatment is less dramatic, indicating a stabilization of the
336 DELLA protein caused by C2/L2 protein. These results were confirmed by immunoblot analyses
337 using an anti-GFP antibody (Figure 7B). GA3 treatment clearly reduced the amount of YFP-GAI
338 when this fusion protein is agroinfiltrated alone, but no significant differences were observed when
339 it is coinfiltrated with any of the C2/L2 expression constructs. As an internal control, a GFP
340 expression construct was agroinfiltrated alone or coinfiltrated with the C2/L2 expression construct.
341 No differences in fluorescence (data not shown) or GFP protein accumulation were detected
342 between treated and untreated plants (Figure 7B)..

343 **Transcriptomic Analysis Reveals a Clear Suppression of Jasmonate Responses in C2** 344 **Plants.**

345 To further characterize the global effects on gene expression induced by C2, we performed a
346 transcriptomic analysis of the transgenic *Arabidopsis* plants expressing TYLCSV C2. Microarray
347 examination reveals 606 genes that were upregulated and 644 that were downregulated in the
348 transgenic plants with a P value below 0.05 compared with control plants. These microarray
349 results were validated by quantitative real-time PCR (see Supplemental Figure 7 online). When
350 we subjected the two groups of genes with altered expression to functional enrichment, we found
351 several biological processes affected by C2-TS, including response to hormone stimulus and
352 defense response (Table 2). As expected, the expression of genes involved in the hormonal

353 responses previously tested is also altered: for example, the gibberellin-responsive GASA4 and
354 GASA5 are downregulated, whereas the ethylene-responsive ATERF4, PDX1L4, and HRE1 are
355 upregulated.

356 Although the number of up- and downregulated genes in the transgenic C2-TS plants is similar,
357 the nonredundant analysis of GO categories did not reveal any specific hormonal response
358 affected among the upregulated genes. Instead, in the subset of repressed genes, it is especially
359 noticeable the presence of processes related to plant defense and response to jasmonates.
360 Among these downregulated genes, some hallmarks of the jasmonates biosynthetic and
361 perception pathways can be found (see Supplemental Table 3 online). When the list of
362 downregulated genes is compared with that of the upregulated genes in a Columbia (Col-0) plant
363 after MeJA treatment (jasmonate-responsive genes) (Nemhauser et al., 2006), the intersection
364 contains 114 common genes (Figure 8). Gene ontology (GO) analysis of these 114 genes reveals
365 that 32 out of 45 (71%) of the GO categories reported as overrepresented for the whole set of
366 downregulated genes in C2-expressing plants are also overrepresented in this intersectional
367 subset (Table 3). On the other hand, intersections between the set of upregulated genes in C2-
368 expressing plants with either up- or downregulated genes in MeJA-treated plants or between the
369 downregulated genes in C2-expressing plants and upregulated genes in MeJA-treated plants give
370 no significant functional terms exceeding the P value cutoff of 0.01. Given that processes related
371 to jasmonates biosynthesis and perception appear to be clearly repressed by C2, we can infer
372 that interference with the jasmonate pathway might to some degree account for the suppression
373 of the defense response, maybe linking this phenotype to the ability of C2 to hinder the activity of
374 the SCFCO11. Taking these results together, we conclude that the inhibition of the jasmonates
375 response is the main process affecting downregulation of transcription in the C2-TS-expressing
376 plants.

377 **Jasmonate Treatment Reduces the Susceptibility to Geminivirus Infection.**

378 Previous results demonstrated that expression of Tomato golden mosaic virus C2 or BCTV L2 in
379 *N. benthamiana* plants produced an enhanced susceptibility to DNA and RNA viruses (Sunter et
380 al., 2001), suggesting that C2/L2 proteins have the ability to suppress host stress or defense
381 responses. Since jasmonate signaling has been extensively implicated in defense responses
382 (reviewed in Bari and Jones, 2009), the changes in hormonal sensitivity observed in the C2/L2
383 transgenic plants could be responsible for this enhanced susceptibility phenotype, suggesting that
384 repression of the jasmonate response could favor viral infection. To determine whether jasmonate
385 response affects geminivirus infection, we inoculated MeJA and mock-treated *Arabidopsis* plants

386 with BCTV. Total DNA was extracted from these samples and subjected to nucleic acid
387 hybridization with a viral probe. Results from symptom evaluation and viral DNA accumulation are
388 presented in Figure 9. The application of exogenous MeJA results in milder symptoms and lower
389 viral DNA accumulation, indicating a disruption of the geminivirus infection by this compound.

390 .

391 **DISCUSSION**

392 **C2, a Protein Required for Virus Infectivity, Interacts with CSN5 and Exerts a Specific Effect** 393 **on CUL1 Rubylation State.**

394 Using TYLCSV C2 as bait protein in a yeast two-hybrid screening, we isolated the Arabidopsis
395 protein CSN5A. Binding assays in yeast and plant confirm C2-CSN5A interaction and
396 demonstrate that this viral protein also binds the tomato ortholog and the Arabidopsis paralog
397 (CSN5B). Interaction experiments using these three CSN5 proteins further demonstrate that they
398 interact with the C2 protein from another begomovirus, TYLCV, and with the homologous protein
399 in the curtovirus BCTV. Taken together, these results suggest that binding to CSN5 is a conserved
400 function of geminivirus C2/L2 protein.

401 Although interactions with components of the CRLs have been described previously for DNA and
402 RNA viruses, only few examples of interactions with the CSN complex have been reported, all
403 limited to animal viruses (Mahalingam et al., 1998; Oh et al., 2006; Tanaka et al., 2006; Hsieh et
404 al., 2007). Even though, as for C2-CSN5, those interactions seem to play a role during virus
405 infection (Oh et al., 2006; Tanaka et al., 2006; Hsieh et al., 2007), the mechanisms proposed
406 point to a redirection of proteosomal degradation rather than to an effect on the derubylating
407 activity of the CSN complex itself.

408 Given that the main biochemical activity of the CSN complex is the derubylation of cullins, we
409 checked the rubylated/derubylated ratio of CUL1, CUL3, and CUL4 in transgenic Arabidopsis
410 lines expressing geminivirus C2/L2 and found that these plants contain a higher proportion of
411 rubylated CUL1; nevertheless, CUL3 and CUL4 rubylation ratio is not altered. Although we cannot
412 rule out the possibility that subtle changes in CUL3 to CUL4 ratio cannot be detected by
413 immunoblots, this result suggests that C2/L2-CSN5 interaction specifically inhibits the
414 derubylation activity of CSN over CUL1. In spite of the fact that the precise mechanism conferring
415 specificity to the action of C2 remains elusive, the interaction between several CSN subunits and
416 SCF components in plants (Schwechheimer et al., 2001) raises the possibility that the reduction

417 in CUL1 derubylation could be the result of the specific interference of C2 with the CSN-SCF
418 binding.

419 Strikingly, even though the CUL3 rubylated/derubylated ratio is not affected by the presence of
420 C2/L2, the transgenic plants expressing these viral genes show a slight increase in the
421 accumulation of CUL3, which seems to be the result of posttranslational regulation, since the level
422 of CUL3 mRNA is reduced in these plants (see Supplemental Figure 8 online). Interestingly, a
423 genetic interaction has been described for CSN5 and CUL3, and CSN5 and CUL3 have been
424 proposed to regulate each other's abundance in an opposite manner (Gusmaroli et al., 2007). In
425 this context, one would expect that C2/L2 interference with CSN function would trigger the same
426 reduction in CUL3 accumulation. However, C2/L2 expression is instead accompanied by an
427 increase in CUL3 abundance. The fact that CUL1 derubylation is affected in the same transgenic
428 lines allows the intriguing possibility that a defective SCF activity could be responsible for CUL3
429 accumulation. Alternatively, a tantalizing, nonexclusive hypothesis could be that C2-mediated
430 blocking of the derubylation of CUL1 could increase the number of CSN complexes available to
431 remove RUB from other cullins, thus reducing CUL3 autodegradation. It has been previously
432 proposed that CSN5A reduced activity could trigger the autoubiquitination and degradation of
433 rubylated CUL1 (Stuttman et al., 2009). However, in spite of a clearly higher
434 rubylated/derubylated CUL1 ratio, we did not observe any destabilization of rubylated CUL1 in
435 either transgenic lines expressing C2/L2 or in *csn5a* mutants, in agreement with previous data
436 indicating that CUL1 is not destabilized in the same *csn5a* background (Gusmaroli et al., 2007).

437 **C2 Affects the Activity of Several SCF Complexes.**

438 Since C2/L2 expression increases the CUL1 rubylated/derubylated ratio, it is reasonable to expect
439 that CUL1-based SCF functions would be compromised in the presence of C2/L2. Transgenic
440 C2/L2 plants share phenotypes with *csn* and *cul1* mutants, including decreased sensitivity to
441 auxins, gibberellins, and jasmonates and enhanced sensitivity to ethylene and ABA in the guard
442 cells, results that are consistent with a general impairment in the activity of several known SCF
443 complexes (SCFTIR1, SCFSLY1, SCFCO11, SCFEFB1/2, and SCFDOR) and the subsequent
444 accumulation of their substrates. The stabilization of YFP-GAI, target of the SCFSLY1 complex,
445 produced when C2/L2 is expressed supports this hypothesis.

446 The observation that the pleiotropic defects of transgenic C2/L2-expressing plants are not as
447 severe as the multifaceted developmental phenotype of *cul1* or *csn5* mutants could be explained
448 by the fact that C2/L2 does not completely impair derubylation but rather hinders it, so that the

449 downstream changes are more subtle. On the other hand, and given that the CSN and the SCF
450 complexes are essential for cell viability, it might also be feasible that the expression of C2/L2
451 could be counterselected, and consequently the expression level of the selected transgenic lines
452 would be low. The fact that overexpression of some C2 proteins from a potato virus X-based
453 vector induces severe developmental changes and the subsequent collapse of the plant (A.P.
454 Luna and E.R. Bejarano, unpublished data) is in agreement with this idea. Another possibility
455 would be that the effect of C2 on the SCF complexes could be specific rather than generalized,
456 as suggested by the transcriptomic data. Curiously, Stuttmann et al. (2009) propose that defects
457 in cullin derubylation may be tolerated without causing obvious physiological defects.

458 **C2 Expression Modulates Jasmonate Responses.**

459 Although transgenic C2/L2 Arabidopsis plants display multiple phenotypes derived from the
460 interference with the function of the SCF complexes, microarray analysis of C2-TS transgenic
461 plants highlighted the jasmonate response as the main SCF-dependent hormone signaling
462 pathway impaired in these plants. Reduction in responsiveness to jasmonates has been reported
463 for transgenic plants expressing antisense RNA of CSN5 (Schwechheimer et al., 2002), as well
464 as for *csn* (Feng et al., 2003) and *cul1* mutants (Ren et al., 2005; Moon et al., 2007). Jasmonates
465 are important plant signaling molecules that mediate biotic and abiotic stress responses as well
466 as several aspects of growth and development. Plants respond to jasmonates by degrading the
467 JAZ family of transcriptional regulators in a SCFCOI1 complex- and a proteasome-dependent
468 manner (Chini et al., 2007; Thines et al., 2007; Sheard et al., 2010). Therefore, it is likely that
469 C2/L2 may alter the jasmonate response through its effect on CUL1 rubylation. However, and
470 given that C2/L2 is a multifunctional protein, we cannot rule out that the observed phenotype
471 might be driven, partially or completely, by a different mechanism, such as the transcriptional
472 activation activity of this viral protein.

473 Several lines of evidence indicate that the suppression of the jasmonate response is required for
474 geminivirus infectivity: (1) MeJA treatment of Arabidopsis plants reduces BCTV infection; (2)
475 infection of Arabidopsis with CaLCuV induces repression of the jasmonate response (Ascencio-
476 Ibáñez et al., 2008); (3) the pathogenesis factor β C1 from DNA β of TYLCCNV can suppress
477 expression of several jasmonate-responsive genes (Yang et al., 2008). Moreover, the fact that
478 both localization of a large number of geminiviruses (e.g., TYLCSV, TYLCV, and BCTV) and
479 jasmonate synthesis occur preferentially in the phloem cells (Stenzel et al., 2003) makes the
480 suppression of the jasmonate response a feasible target during infection. This suppression could
481 have a direct effect in virus movement or replication by leading to several changes in the plant

482 advantageous for the virus, such as the inhibition of the synthesis of secondary metabolites
483 deleterious for viral replication or movement (e.g., phenylpropanoids; (Kandan et al., 2002; Matros
484 and Mock, 2004), or might be aimed at circumventing phloem cell wall in growth development
485 (Amiard et al., 2007).

486

487 Additionally, the interference with the jasmonate signaling may have an impact on the viral insect
488 vector. Jasmonates are the hormones mediating plant defense against insects and could
489 therefore be indirectly affecting geminivirus spread. Both TYLCSV and TYLCV are transmitted by
490 the whitefly *Bemisia tabaci*, and it has been described that whitefly nymphs trigger the expression
491 of jasmonate-responsive genes, which are important in slowing nymphal development (Kempema
492 et al., 2007; Valenzuela-Soto et al., 2010). Through the suppression of the jasmonate response,
493 the virus might be accelerating its vector's cycle, thus enhancing its own spread. On the other
494 hand, this suppression could also prevent the synthesis of secondary metabolites that could
495 interfere with the interaction between plant and insect (Bleeker et al., 2009).

496 **C2/L2 Might Facilitate Co-Option of the SCF-Mediated Ubiquitination.**

497 According to our results, it seems that C2/L2 would be capable of hindering the activity of several
498 SCF complexes in the plant cell, presumably conferring some biological advantage for the viral
499 infection, such as suppression of hormone-mediated plant defense responses. It is an appealing
500 hypothesis, however, that the virus might be not only impairing the function of the SCF complexes,
501 but rather also redirecting them toward certain target proteins whose degradation would be
502 advantageous for the viral infection. The fact that the overexpression of a given F-box protein can
503 circumvent the general malfunction of the SCF complexes (Denti et al., 2006; Stuttmann et al.,
504 2009) raises the idea that geminiviruses could be co-opting the SCF-mediated ubiquitination
505 pathway for their own advantage through the promotion of the expression of selected adaptor
506 subunits. It would be interesting to look for F-box proteins upregulated during geminivirus infection
507 or in heterologous expression of geminiviral proteins to localize possible targets of this theoretical
508 mechanism.

509

510 Some plant viruses have been shown to co-opt the SCF machinery by encoding their own viral F-
511 box proteins, which are assembled into plant SCF complexes (Baumberger et al., 2007;
512 Bortolamiol et al., 2007; Lageix et al., 2007), triggering the ubiquitination of plant proteins that

513 interfere with viral infection. Thus, it would be a tempting hypothesis that, to maximize the effect
514 of their encoded F-box proteins, promoting their efficient incorporation in the maximum possible
515 number of SCF complexes, these plant viruses might have developed means to interfere with the
516 assembly/disassembly cycle of SCF complexes, which is based in rubylation and derubylation.

517

518 In summary, viruses typically encode a few multifunctional proteins that enable them to redirect
519 the host replication and transcriptional machineries to viral templates, reprogram host cells to
520 provide an environment favorable for the viral infection, and counteract host defenses. The results
521 obtained in this work unveil a powerful strategy used by geminiviruses, which involves the
522 interaction with a hub regulator of protein ubiquitination, a mechanism that could allow the virus
523 to trigger wide changes in the cellular homeostasis. Additional studies will be required to further
524 dissect the molecular mechanisms underlying this strategy and to determine whether this is a
525 generalized tactic for viruses.

526

527 **MATERIALS AND METHODS**

528 **Microorganisms and general methods.**

529 Manipulations of *Escherichia coli* and *Saccharomyces cerevisiae* strains and nucleic acids were
530 performed according to standard methods (Ausubel et al., 1998; Sambrook and Russell, 2001).
531 *E. coli* strain DH5- α was used for subcloning. All PCR-amplified fragments cloned in this work
532 were fully sequenced. *Agrobacterium tumefaciens* GV3101 strain was used for the agroinfiltration
533 assays, and LBA4404 was used for plant transformation. *S. cerevisiae* strain pJ696 (MATa, trp1-
534 901, leu2-3,112, ura3-52, his3-200, gal4 Δ , gal80 Δ , GAL2-ADE2, LYS2::GAL1-HIS3, met2::GAL7-
535 lacZ), a derivative of PJ69-4A (James et al., 1996), was used for the two-hybrid experiments.
536 Plant DNA gel blots were performed as described by Castillo et al. (2004).

537 **Plant Materials and Growth Conditions**

538 Wild-type *Arabidopsis thaliana* used in this study is the Col ecotype. Seeds were surface sterilized
539 and sown on Murashige and Skoog (MS) agar plates with 30 g/liter sucrose. Plates were cold
540 treated for 2 to 6 d at 4°C. Seedlings were grown at 20°C under fluorescent white light (fluence
541 rate of 40 to 60 $\mu\text{mol m}^{-2} \text{s}^{-1}$) with a 16-h-light/8-h-dark photoperiod. For far-red light treatments,
542 seedlings were grown under continuous far-red light (fluence rate of 110 $\mu\text{mol m}^{-2} \text{s}^{-1}$). For dark-
543 grown seedlings, plates were wrapped in several layers of aluminum foil.

544 For root growth inhibition assays, MS plates were placed in a vertical orientation for 5 d, and
545 seedlings were then transferred to MS plates containing the tested hormone. Root length was
546 scanned 5 d later using ImageJ software (<http://rsb.info.nih.gov/ij>). The hormones and
547 concentrations used in the root growth inhibition assays were the following: 2,4-D (Duchefa
548 Biochemie; 0.1 μ M), MeJA (Duchefa Biochemie; 50 or 100 μ M), GA3 (Duchefa Biochemie; 0.2
549 μ M), and ACC (Sigma-Aldrich A3903; 1 μ M).

550 MeJA treatments for the infection experiments were as follows: a 50 μ M MeJA solution or mock
551 solution (containing 50 μ M ethanol) were applied to 4-week-old Arabidopsis plants by spray every
552 other day from 1 d before the inoculation to 28 DAI.

553 For the agroinfiltration experiments, *N.benthamiana* plants were grown in soil at 22°C in long-day
554 conditions (16-h-light/8-h-dark photoperiod). For the root growth inhibition assays, wild-type and
555 transgenic C2 *N. benthamiana* seeds were surface sterilized and sown on MS agar plates, and
556 the seedlings were subjected to the corresponding treatments described for Arabidopsis.

557 The *csn5a-1* mutant (SALK_063436 line) was previously described (Gusmaroli et al., 2007).

558 For the transcriptomic analysis, T2 seedlings were grown on MS with kanamycin for 7 d and then
559 were treated with hormone-containing or mock solutions at the indicated concentrations for the
560 indicated time: 1 μ M 2,4D, 1 h; 50 μ M MeJA, 10 h; 1 μ M GA3, 1 h; 10 μ M ACC, 1 h. Three
561 independent replicates were performed. For these analyses, transgenic kanamycin-resistant
562 plants containing with an expression cassette to express the firefly luciferase (LUC) reporter gene
563 (Murray et al., 2002) were used as the control, and all seedlings were selected in kanamycin.
564 Previously, the hormonal responses of the LUC plants were proved to be identical to those of the
565 wild-type in the aforementioned assays.

566 **Drought Tolerance Test**

567 For the drought tolerance test, plants were initially grown on soil under a normal watering regime
568 for 6 to 7 weeks. Watering was then halted and observations were taken after a further 10 d
569 without water supply.

570 **Weight Loss Measurements**

571 For weight loss measurements, rosette leaves from 4-week-old plants were detached, placed on
572 weighing dishes, and allowed to dry at room conditions. Weight of the samples was recorded at
573 0, 0.5, 1, 2, 3, and 4 h, and the percentage of initial weight was calculated for each point.

574 **Stomatal Aperture Measurements**

575 Rosette leaves from 4- to 5-week-old plants were exposed to white light for 2 h (fluence rate of
576 40 to 60 $\mu\text{mol m}^{-2} \text{s}^{-1}$) while submerged in a solution containing 50 mM KCl, 10 μM CaCl₂, 0.01%
577 Tween 20, and 10 mM MES-KOH, pH 6.15, to induce stomatal aperture. Subsequently, 5 μM ABA
578 (Sigma-Aldrich A4906) or mock solution was added to the buffer, and the samples were incubated
579 under the same conditions for 1 h. Epidermal peels were stained with toluidine blue and observed
580 under the microscope (TCS NT; Leica). Stomatal aperture was measured using ImageJ software.

581 **Plasmids and Cloning**

582 TYLCSV C2T2C mutant virus was generated by two-sided splicing by overlap extension (Ho et
583 al., 1989). Primers pairs C2T2C-F/Fragment2C2T2C -R and C2T2C-R/ Fragment1C2T2C -F
584 were used in the two initial PCR reactions; subsequent amplification used primers
585 Fragment1C2T2C -F/ Fragment2C2T2C -R. The PCR product was cloned into the EcoRV site
586 of pBluescript SKII+ (Stratagene) to yield pBSSK-TYA14NdeI/NcoI. An NdeI/NcoI fragment
587 containing the wild-type C2 start codon in pGreenTYA14 was replaced by the NdeI/NcoI fragment
588 in pBSSK-TYA14NdeI/NcoI to generate pGreenTYA14C2T2C.

589 For the yeast two-hybrid constructs, cDNA from Arabidopsis and tomato (*Solanum lycopersicum*)
590 were generated from total RNA extracted from seedlings and leaves respectively. One microgram
591 of total RNA was used for first-strand cDNA synthesis using oligo(dT) primers and SuperScript II
592 reverse transcriptase reagent (Invitrogen) following the manufacturer's instructions. Arabidopsis
593 CSN5A 44-357 and CSN5B 44-358 and tomato JAB (CSN5)57-357 were PCR amplified and
594 cloned into pGADT7 vector (Clontech). Full C2/L2 open reading frame (ORF) from TYLCSV
595 (accession number L27708), TYLCV (accession number AF071228), and BCTV (accession
596 number AF379637) were amplified by PCR and cloned into pGBKT7 vector (Clontech).

597 For the BiFC experiments, cDNA from Arabidopsis and tomato were generated as indicated for
598 the yeast two-hybrid constructs. Arabidopsis CSN5 and tomato JAB ORFs were PCR amplified
599 and cloned into the pENTR/D-TOPO vector. Full C2/L2 ORF from TYLCSV, TYLCV, and BCTV
600 was amplified by PCR and cloned into the pENTR/D-TOPO vector. Cloned ORFs were inserted
601 by LR reaction (Invitrogen) into the binary pBiFP vectors pBiFP2 and pBiFP3 (de Lucas et al.,
602 2008) containing the N- or C-terminal fragments of the eYFP fluorescent protein (NYFP and
603 CYFP). The resulting constructs were used to transform *A. tumefaciens* GV3101.

604 For plant transformation and transient expression, PCR fragments containing the C2/L2 full ORF
605 of TYLCSV, TYLCV, and BCTV were blunt-cloned in pBluescript SKII+ (Stratagene) (TYLCV C2
606 and BCTV L2) or cloned into the HpaI site of pSXS1 (M.A. Sánchez-Durán, M.B. Dallas, J.T.
607 Ascencio-Ibañez, M.I. Reyes, M. Arroyo-Mateos, J. Ruiz-Albert, L. Hanley-Bowdoin, and E.R.
608 Bejarano, unpublished data) (TYLCSV C2) to yield pC2TM, pL2BC, and pSXC2TS, respectively.
609 Fragments containing TYLCV C2 and BCTV L2 full ORFs were obtained from pC2TM and pL2BC
610 by HpaI/KpnI digestion and subcloned in the HpaI/KpnI sites of pBINX (M.A. Sánchez-Durán, M.B.
611 Dallas, J.T. Ascencio-Ibañez, M.I. Reyes, M. Arroyo-Mateos, J. Ruiz-Albert, L. Hanley-Bowdoin,
612 and E.R. Bejarano, unpublished data) to yield pBINX-C2-TM and pBINX-L2-BC. A fragment
613 comprising an expression cassette containing the TYLCSV C2 full ORF was obtained from
614 pSXC2TS by XbaI digestion and subcloned into the XbaI site of the binary vector pBIN+ (van
615 Engelen et al., 1995) to yield pBIN-C2-TS.

616 For the subcellular localization study, TYLCSV C2 ORF was fused to GFP at its N terminus, and
617 the fusion protein or GFP alone was cloned under the control of the 35S promoter in a pBINX1
618 (M.A. Sánchez-Durán et al., unpublished data) to yield pBINX1-GFP-C2 and pBINX1-GFP. GFP
619 ORF was PCR amplified from pSMGFP (Davis and Vierstra, 1998).

620 Supplemental Table 1 online contains all the oligonucleotides used in this study. Supplemental
621 Table 2 online summarizes the engineering of the plasmids used in this work.

622 **Phylogenetic Analysis.**

623 Amino acid plant CSN5 homolog proteins were aligned with ClustalW
624 (<http://www.ebi.ac.uk/clustalw/index.html>). Afterwards, the alignment was checked and manually
625 adjusted. The resultant aligned sequences (see Supplemental Data Set 1 online) were used to
626 construct a phylogenetic tree (unrooted) using neighbor-joining clustering based on pairwise
627 mean character differences conducted in SEAVIEW (SEAVIEW 4.2.12; [http://pbil.univ-](http://pbil.univ-lyon1.fr/software/seaview.html)
628 [lyon1.fr/software/seaview.html](http://pbil.univ-lyon1.fr/software/seaview.html); Gouy et al., 2010). Statistical support of branches was assessed
629 by bootstrap analyses using 1000 resamples of the data matrix.

630 **Yeast Two-Hybrid Assay.**

631 The yeast strain PJ696, which contains the reporter genes lacZ, HIS3, and ADE2, was used in
632 the two-hybrid assays (Fields and Song, 1989). Assays were performed as described (Castillo et
633 al., 2004). Yeast were cotransformed and selected for bait and prey plasmids, as described Yeast
634 Protocols Handbook (Clontech Laboratories).

635 **BiFC Assays.**

636 Different combination of the *A. tumefaciens* clones expressing the fusion proteins (NYFP-
637 CSN5/CYFP-C2/L2 or NYFP-C2/L2/CYFP-CSN5) were coinfiltrated into the abaxial surface of 2-
638 to 3-week-old *N. benthamiana* plants as described (Voinnet et al., 2003). The p19 protein of
639 Tomato bushy stunt virus (pBIN61-p19, kindly provided by Olivier Voinnet, Strasbourg, France)
640 was used to suppress gene silencing. *A. tumefaciens* strains containing the pBiFP constructs or
641 the p19 plasmid were at a D 600 ratio of 1:1:1 for infiltration. Fluorescence was visualized in
642 epidermal cell layers of the leaves after 3 d of infiltration using a Leica DMR confocal microscope.

643 **Subcellular Localization**

644 *A. tumefaciens* GV3101 was transformed with pBIN1-GFP-C2 or pBIN1-GFP plasmids and
645 coinfiltrated with p19 as described above. *A. tumefaciens* strains containing pBINX1-GFP-C2 or
646 pBIN1-GFP (as a control) and the p19 silencing plasmid were at a D 600 ratio of 1:1 for infiltration.
647 Fluorescence was visualized in epidermal cell layers of the leaves after 3 d of infiltration using a
648 Leica DMR fluorescence microscope.

649 **Plant Transformation**

650 *Arabidopsis* transformation was performed by floral dip (Clough and Bent, 1998) using *A.*
651 *tumefaciens* GV3101 containing pBIN-C2-TS, pBINX-C2-TM, or pBINX-L2-BC. Transformants
652 were selected with kanamycin (50 µg/mL). *N. benthamiana* plants were transformed with pBIN-
653 C2-TS as described by Morilla et al. (2006). Ten independent lines per construct were selected
654 and subjected to expression analysis by RNA gel blot. Unless otherwise indicated, T2 seeds from
655 the lines C2-TS 9, C2-TM 1, and L2-BC 4 were used in this work. Further information about the
656 transgenic lines is provided in Supplemental Figure 3 online.

657 **Transient Expression Assays**

658 For the *in vivo* degradation assay, the YFP-GAI construct (kindly provided by David Alabadí,
659 Instituto de Biología Molecular y Celular de Plantas, Valencia, Spain) and the C2/L2 expression
660 constructs were used to transform *A. tumefaciens* GV3101. Three days after infiltration, the
661 agroinfiltrated leaves were sprayed with a 100 µM GA3 solution or with mock solution containing
662 the GA3 solvent (ethanol). Fluorescence was visualized 1 to 2 h later using an epifluorescence
663 Leica microscope MZ FLIII.

664 **Immunoblot and Gel Filtration Assays.**

665 Immunoblot and gel filtration analyses of plant extracts were performed as described by
666 Gusmaroli et al. (2004). In all cases in which equal loading was required, the same samples were
667 probed with α -RPN6 to confirm equal loading. For quantitative experiments, multiple exposures
668 were obtained to assure that the film was not saturated. The antibodies used in this study are as
669 follows: α -CUL1 (Wang et al., 2002), α -CUL3 (Figuroa et al., 2005), α -CUL4 (Chen et al., 2006),
670 α -CSN5 (Kwok et al., 1998), α -RBX1 (Schwechheimer et al. 2002), α -SKP1 (Gray et al., 1999),
671 and α -GFP (kindly provided by Olivier Voinnet, Strasbourg, France).

672 **Quantitative Real-Time PCR.**

673 Primer pairs for real-time PCR were designed using Primer 3 software
674 (<http://frodo.wi.mit.edu/primer3/>; see Supplemental Table 1 online). Gene-specific primers were
675 chosen so that the PCR products were 100 to 300 bp. Total RNA was extracted using RNeasy
676 Plant Mini Kit (Qiagen) and treated on column with Dnase (Qiagen). One microgram of total RNA
677 was used for first-strand cDNA synthesis using oligo(dT) primers and SuperScript II reverse
678 transcriptase reagent (Invitrogen) following the manufacturer's instructions. For real-time PCR,
679 the reaction mixture consisted of cDNA first-strand template, primer mix (5 μ mol each) and SYBR
680 Green Master Mix (Quanta Biosciences) in a total volume of 25 μ L. The PCR conditions were as
681 follows: 10 min at 95°C and 40 cycles of 30 s at 95°C and 30 s at 60°C. The reactions were
682 performed using a Rotor-Gene real time cycler (Qiagen). A relative quantification real-time PCR
683 method was used to compare expression of the genes in transgenic versus nontransgenic line
684 (Panchuk et al., 2002). Relative quantification describes the change in expression of the target
685 gene in a test sample relative to calibrator sample. Actin was used as the internal control. The
686 sample of LUC transgenic plants was used as the calibrator, with the expression level of the
687 sample set to 1. Each data point is the mean value from three experimental replicate
688 determinations. Each cDNA sample used is a mixture from three biological replicates at a ratio of
689 1:1:1.

690 **Transcriptomic Studies.**

691 Microarray analysis was performed at the Unité de Recherche en Génomique Végétale (Evry,
692 France) using the CATMA arrays, containing 24,576 gene-specific tags corresponding to 22,089
693 genes from Arabidopsis (Crowe et al., 2003; Hilson et al., 2004). For each point, three
694 independent biological replicates were produced. For each biological repetition, RNA samples
695 were obtained by pooling RNAs from 8 to 10 plants. Samples were collected on plants at 1.10 to
696 1.12 developmental growth stages (Boyes et al., 2001), cultivated in MS plus kanamycin. Total

697 RNA was isolated from three replicates of the 35S:LUC and transgenic C2-TS seedlings using
698 TRIzol (Invitrogen) and subsequently cleaned using the RNeasy MinElute cleanup kit (Invitrogen).
699 RNA quantity and quality were assessed with a Nanodrop ND-1000 spectrophotometer (Labtech)
700 and an Agilent 2100 bioanalyzer (Agilent Technologies), respectively. For each comparison and
701 each biological replicate, a dye-swap was performed (i.e., six hybridizations per comparison). The
702 labeling of cRNAs with Cy3-dUTP or Cy5-dUTP (Perkin-Elmer-NEN Life Science Products), the
703 hybridization to the slides, and the scanning were performed as described by Lurin et al. (2004).

704 For each array, the raw data comprised the logarithm of median feature pixel intensity at
705 wavelengths 635 nm (red) and 532 nm (green), and no background was subtracted. An array-by-
706 array normalization was performed to remove systematic biases. First, spots considered badly
707 formed features were excluded. Then, a global intensity-dependent normalization using the loess
708 procedure (see Yang and Speed, 2002) was performed to correct the dye bias. Finally, for each
709 block, the log-ratio median calculated over the values for the entire block was subtracted from
710 each individual log-ratio value to correct effects on each block, as well as print tip, washing, and/or
711 drying effects.

712 Differential analysis was based on the log ratios averaged on the dye-swap: the technical
713 replicates were averaged to get one log-ratio per biological replicate, and these values were used
714 to perform a paired t test. For each spot, the empirical variance was calculated and then a trimmed
715 variance was calculated from spots, which did not display extreme variance. The spots that were
716 excluded were those with a specific variance/common variance ratio smaller than the α -quantile
717 of a χ^2 distribution of two degree of liberty or greater than the $1-\alpha$ -quantile of a χ^2 distribution of
718 two degree of liberty with α equal to 0.0001 (the same order of magnitude as the probe number).
719 The raw P values were adjusted by the Bonferroni method, which controls the family-wise error
720 rate to keep a strong control of the false positives in a multiple-comparison context. We
721 considered as being differentially expressed the spots with a Bonferroni P value ≤ 0.05 . A
722 detailed description of the normalization step and of the variance modeling used in the differential
723 analysis is available in Gagnot et al. (2008).

724 **Geminivirus Infection Assays.**

725 Twenty plants were agroinoculated with pGreenTYA14 (binary vector containing a partial dimer
726 of TYLCSV; see Supplemental Table 2 online) or pGreenTYA14C2T2C (the same construct
727 carrying a T-C transition in the start codon of the C2 ORF). For control, five plants were mock

728 inoculated with *A. tumefaciens* harboring the empty binary vector pGreen-0229 (Hellens et al.,
729 2000). Symptoms were evaluated every week until 42 DAI. Samples were taken at 21 DAI.

730 BCTV viral infections of *Arabidopsis* were performed by agroinoculation using wild-type virus
731 (Briddon et al., 1989). Symptoms were evaluated every week until 28 DAI. Samples were taken
732 at 28 DAI.

733 Viral DNA accumulation was quantified by DNA gel blot hybridization of total plant DNA. Two
734 micrograms of total DNA were used. Membranes were hybridized with TYLCSV or BCTV
735 radiolabeled probes. Viral DNA accumulation was quantified by phosphorimager analyses of DNA
736 gel blots and normalized to genomic DNA

737 **Accession Numbers.**

738 *Arabidopsis* Genome Initiative locus identifiers for the genes used in this article are as follows:
739 AT1G22920 (CSN5A), AT1G71230 (CSN5B), AT4G02570 (CUL1), AT1G26830 (CUL3A),
740 AT1G69670 (CUL3B), AT5G46210 (CUL4), AT3G23240 (ERF1), AT2G40940 (ERS1),
741 AT1G73590 (PIN1), At3g15540 (IAA19), At5g45460 (MFC19.13), At5g64120 (MHJ24.10),
742 At2G06050 (OPR3), and At3G16470 (JR1). Microarray data from this article were deposited at
743 Gene Expression Omnibus (<http://www.ncbi.nlm.nih.gov/geo/>) under accession number
744 GSE24475 and at CATdb (<http://urgv.evry.inra.fr/CATdb/>; Project AU07-12_GeminiSelSup)
745 according to the Minimum Information About a Microarray Experiment standards.

746 **SUPPLEMENTAL DATA.**

747 The following materials are available in the online version of this article.

748 Supplemental Figure 1. Infection of *N. benthamiana* Plants with TYLCSV Wild Type or C2T2C
749 Mutant.

750 Supplemental Figure 2. Comparison of CSN5 from Several Plant Species.

751 Supplemental Figure 3. Characterization of the Transgenic *Arabidopsis* Lines Expressing C2/L2.

752 Supplemental Figure 4. CUL1 and CUL3 Protein Accumulation in Transgenic *Arabidopsis* Lines
753 Expressing C2/L2.

754 Supplemental Figure 5. Hypocotyl Length of 9-d-Old Dark-Grown Transgenic C2-TS, C2-TM, and
755 L2-BC or Wild-Type *Arabidopsis* Seedlings.

756 Supplemental Figure 6. Reduced Response to Hormones in Transgenic Arabidopsis and N.
757 benthamiana Plants Expressing C2.

758 Supplemental Figure 7. Evaluation of the Expression of Two Differentially Expressed Genes in
759 Transgenic C2-TS Arabidopsis Plants for Microarray Validation.

760 Supplemental Figure 8. Relative Expression of CUL3 in C2-TS, C2-TM, and L2-BC or Control
761 Arabidopsis Seedlings Determined by Quantitative Real-Time PCR.

762

763 Supplemental Table 1. Oligonucleotides Used in This Study.

764 Supplemental Table 2. Plasmids Generated in This Work.

765 Supplemental Table 3. Hallmark Genes of the Jasmonate Response Downregulated in the
766 Microarray of C2-TS Transgenic Plants.

767 Supplemental Data Set 1. Text File of Alignment Corresponding to Phylogenetic Analysis in
768 Supplemental Figure 2.

769 **ACKNOWLEDGMENTS**

770 We thank David Alabadi for providing the YFP-GAI construct, Salome Prat for the BiFP vectors,
771 and Olivier Voinnet for the anti-GFP antibody and pBIN61-p19. We thank Miguel A. Botella,
772 Vicente Rubio, Jae Hoon Lee, and Ning Wei for helpful suggestions and discussions and Alberto
773 Macho, Mayte Duarte, David Navas, and Marie-Laure Martin-Magniette for technical assistance.
774 This research was supported by a grant from the Spanish Ministerio de Ciencia y Tecnología
775 (AGL2007-66062-C02-02/AGR) and by National Science Foundation Grant MCB-0929100 to
776 X.W.D. R.L.-D. was awarded a Predoctoral Fellowship from the Spanish Ministerio de Educación
777 y Cultura and an EMBO Short-Term Fellowship (ASTF 234-2007). A.P.L was awarded a
778 Predoctoral Fellowship from the Junta de Andalucía., ~~raising the tantalizing idea that the~~
779 ~~identification of the molecular mechanisms underlying these viral effects could unlock yet~~
780 ~~unknown stress tolerance strategies and pave the way for the generation of stress resilient plants.~~
781 ~~Geminiviruses are viruses with small circular, single-stranded-DNA genomes that infect a broad~~
782 ~~range of plants. The geminivirus *Tomato yellow leaf curl virus* (TYLCV) is a main causal agent of~~
783 ~~Tomato yellow leaf curl disease (TYLCD), one of the most devastating viral diseases affecting~~
784 ~~tomato crops in tropical and temperate areas worldwide. Interestingly, infection by TYLCV has~~
785 ~~been shown to alleviate heat stress responses in tomato (reviewed in (Gorovits et al. 2019)). Here~~

786 we show that infection by TYLCV enhances drought tolerance in tomato and *Nicotiana*
787 *benthamiana*, and that the virus encoded protein C4 is the viral determinant conferring drought
788 tolerance in *Arabidopsis* through an ABA independent mechanism. In order to determine whether
789 the infection by TYLCV could affect drought tolerance in its natural host, tomato, as well as in the
790 model *Solanaceae* species *N. benthamiana*, we inoculated plants with a TYLCV infectious clone
791 by agroinoculation, and subjected half of the infected plants to drought treatment at 21 days post-
792 inoculation. Interestingly, TYLCV-infected plants from both species, wilted more slowly after the
793 drought treatment and displayed milder drought related symptoms, suggesting that the presence
794 of TYLCV promotes drought tolerance (Figures 1a and 1b).

795 In order to find out if one of the virus encoded proteins is sufficient to confer the observed
796 enhanced drought tolerance, we subjected transgenic *Arabidopsis* lines constitutively expressing
797 the viral genes (C2, C3, C4, V2, and CP) from a 35S promoter to drought treatment and evaluated
798 their performance; constitutive expression of Rep renders plants non viable, hence this protein
799 was not included in this study. Drought did not affect expression of the transgenes (data not
800 shown). As shown in Figure 1c, among the viral proteins tested, only C4 had an impact on the
801 tolerance of *Arabidopsis* to drought: 35S:C4 transgenic plants stayed green and turgid following
802 water deprivation, while transgenic plants expressing other viral proteins or control plants wilted
803 and eventually died.

804 C4 localizes both at the plasma membrane (PM) and in chloroplasts (Rosas-Díaz et al. 2018).
805 Given this double subcellular localization pattern, we wondered whether C4 is promoting drought
806 tolerance through its specific activity at one of these two locations. In order to answer this question,
807 we tested the drought tolerance of transgenic *Arabidopsis* plants expressing the mutated C4
808 version, C4_{G2A}, which accumulates exclusively in chloroplasts (Rosas-Díaz et al. 2018). Despite
809 showing transgene expression levels similar to those observed in 35S:C4 plants, 35S:C4_{G2A}
810 plants displayed sensitivity to drought comparable to that of wild type plants (Figure 1d), indicating
811 that chloroplastic C4 is not sufficient to confer drought tolerance and suggesting that its plasma
812 membrane localization is required for this effect.

813 Transgenic expression of C4 in *Arabidopsis* has been recently shown to interfere with xylem
814 patterning in the root (Fan et al.). With the purpose to determine whether the effect of C4 on
815 drought tolerance could be uncoupled from its impact on xylem patterning, we evaluated the
816 drought tolerance of *SCR:C4* transgenic *Arabidopsis* plants, which express C4 under the
817 endodermis specific *SCARECROW* (*SCR*) promoter but display xylem patterning defects similar
818 to those observed in 35S:C4 plants (Fan et al.). As shown in Figure 1e, *SCR:C4* plants did not

Código de campo cambiado

819 show enhanced drought tolerance, indicating that the effects of C4 on xylem patterning and
820 drought tolerance are independent, and that the latter requires expression of C4 outside of the
821 SCR expression domain.

822 Since ABA is the main hormone regulating drought responses in plants, we decided to assess
823 the effect of C4 on ABA accumulation and responses by: a) quantifying ABA accumulation and
824 expression of ABA responsive genes in basal and drought conditions in wild-type, 35S:C4, and
825 35S:C4_{G2A} plants; and b) evaluating the ability of 35S:C4 and 35S:C4_{G2A} plants to respond to
826 exogenously applied ABA, compared to the wild-type control. Interestingly, C4 expressing plants
827 did not differ from wild-type plants in any of the readouts measured (Figure 1f, 1g and 1h,
828 respectively). Taken together, these results indicate that C4 does not significantly affect the ABA
829 pathway, and therefore must be promoting drought tolerance in an ABA-independent manner.

830 Considering the current prospects of growth in world population, increasing crop yield is a
831 cornerstone to guarantee food security. In a context of climate change, boosting agricultural
832 productivity will necessarily entail generating not only high-yielding, but also stress-resistant crops.
833 While traditional breeding has provided valuable solutions in the past, the current scenario makes
834 it essential to explore alternative approaches, which may allow to narrow the temporal gap
835 between identification of a beneficial trait and its implementation in the field. The study of
836 extremophile species has been suggested as having the potential to unlock novel sources of
837 resistance (Zhang et al. 2018). Similarly, unravelling the physiological and molecular mechanisms
838 underlying the beneficial effects of virus infection on abiotic stress tolerance may uncover new
839 approaches to generate stress tolerance, informing strategies to speed up the generation of crop
840 varieties with increased resilience to abiotic stresses.

841 Our results demonstrate that the virus encoded plasma membrane localized C4 protein is
842 sufficient to confer drought resistance to Arabidopsis plants (Figure 1c). At the plasma membrane,
843 C4 interacts with the receptor like kinases BAM1 and BAM2; however, BAM1, which is inhibited
844 by C4 (Rosas-Díaz et al. 2018; Fan et al.), plays a positive role in the response to drought
845 (Takahashi et al. 2018). More importantly, the effect of C4 on drought tolerance seems
846 independent of ABA (Figure 1f, 1g, 1h). Taken together, these facts support the idea that C4
847 confers drought tolerance through a BAM1-independent, yet-to-be-identified mechanism.

848 Viruses have been shown to enhance drought tolerance through the promotion of salicylic acid
849 (SA) signalling (Aguilar et al. 2017). C4 expressing plants, however, do not overaccumulate SA,
850 and do not display increased expression of SA marker genes (data not shown), indicating that the

851 ~~events underlying the effect of C4 on drought stress tolerance are different to the ones previously~~
852 ~~described for other viruses (Xu et al. 2008; Westwood et al. 2012; Aguilar et al. 2017).~~

853 ~~In summary, our findings demonstrate that C4 from TYLCV increases plant drought tolerance in~~
854 ~~an ABA-independent manner through a mechanism that relies on the presence of this protein at~~
855 ~~the plasma membrane. Considering the dramatic increase in survival upon water withholding~~
856 ~~mediated by C4 and the fact that this effect is independent of well-known hormonal pathways~~
857 ~~linked to drought stress, we believe this discovery to entail great biotechnological potentiality.~~
858 ~~Future efforts will focus on unravelling the molecular events underpinning the C4 triggered~~
859 ~~enhanced tolerance to limited water availability: the identification of the viral drought tolerance-~~
860 ~~promoting strategy could open up new avenues to explore in the engineering of the highly sought-~~
861 ~~after drought-tolerant crops.~~

862

863

864 **LITERATURE CITED**

- 865 1. Agudelo-Romero P. Carbonell P. de la Iglesia F. Carrera J. Rodrigo G. Jaramillo
866 A. Pérez-Amador M.A. Elena S.F. (2008). Changes in the gene expression profile of
867 Arabidopsis thaliana after infection with Tobacco etch virus. Virol. J. 5: 92.
- 868 2. Amiard V. Demmig-Adams B. Mueh K.E. Turgeon R. Combs A.F. Adams W.W. III
869 (2007). Role of light and jasmonic acid signaling in regulating foliar phloem cell wall ingrowth
870 development. New Phytol. 173: 722–731.
- 871 3. Aronson M.N. Meyer A.D. Györgyey J. Katul L. Vetten H.J. Gronenborn B.
872 Timchenko T. (2000). Clink, a nanovirus-encoded protein, binds both pRB and SKP1. J. Virol. 74:
873 2967–2972.
- 874 4. Ascencio-Ibáñez J.T. Sozzani R. Lee T.J. Chu T.M. Wolfinger R.D. Cella R. Hanley-
875 Bowdoin L. (2008). Global analysis of Arabidopsis gene expression uncovers a complex array of
876 changes impacting pathogen response and cell cycle during geminivirus infection. Plant Physiol.
877 148: 436–454.
- 878 5. Ausubel F. Brent R. Kingston R. Moore D. Seidman J. Smith J. Struhl K. (1998).
879 Current Protocols in Molecular Biology. (New York: John Wiley & Sons).

- 880 6. Baliji S. Sunter J. Sunter G. (2007). Transcriptional analysis of complementary sense
881 genes in spinach curly top virus and functional role of C2 in pathogenesis. *Mol. Plant Microbe*
882 *Interact.* 20: 194–206.
- 883 7. Bari R. Jones J.D. (2009). Role of plant hormones in plant defence responses. *Plant*
884 *Mol. Biol.* 69: 473–488.
- 885 8. Baumberger N. Tsai C.H. Lie M. Havecker E. Baulcombe D.C. (2007). The
886 Ploverovirus silencing suppressor P0 targets ARGONAUTE proteins for degradation. *Curr. Biol.*
887 17: 1609–1614.
- 888 9. Bleeker P.M. Diergaarde P.J. Ament K. Guerra J. Weidner M. Schütz S. de Both
889 M.T. Haring M.A. Schuurink R.C. (2009). The role of specific tomato volatiles in tomato-whitefly
890 interaction. *Plant Physiol.* 151: 925–935.
- 891 10. Bortolamiol D. Pazhouhandeh M. Marrocco K. Genschik P. Ziegler-Graff V. (2007).
892 The Ploverovirus F box protein P0 targets ARGONAUTE1 to suppress RNA silencing. *Curr. Biol.*
893 17: 1615–1621.
- 894 11. Boyes D.C. Zayed A.M. Ascenzi R. McCaskill A.J. Hoffman N.E. Davis K.R. Görlach
895 J. (2001). Growth stage-based phenotypic analysis of Arabidopsis: A model for high throughput
896 functional genomics in plants. *Plant Cell* 13: 1499–1510.
- 897 Google ScholarPubMedWorldCat
- 898 12. Briddon R.W. Watts J. Markham P.G. Stanley J. (1989). The coat protein of beet curly
899 top virus is essential for infectivity. *Virology* 172: 628–633.
- 900 13. Castillo A.G. Kong L.J. Hanley-Bowdoin L. Bejarano E.R. (2004). Interaction between
901 a geminivirus replication protein and the plant sumoylation system. *J. Virol.* 78: 2758–2769.
- 902 14. Chen H. Shen Y. Tang X. Yu L. Wang J. Guo L. Zhang Y. Zhang H. Feng S.
903 Strickland E. Zheng N. Deng X.W. (2006). Arabidopsis CULLIN4 forms an E3 ubiquitin ligase
904 with RBX1 and the CDD complex in mediating light control of development. *Plant Cell* 18: 1991–
905 2004.
- 906 15. Chini A. Fonseca S. Fernández G. Adie B. Chico J.M. Lorenzo O. García-Casado
907 G. López-Vidriero I. Lozano F.M. Ponce M.R. Micol J.L. Solano R. (2007). The JAZ family
908 of repressors is the missing link in jasmonate signalling. *Nature* 448: 666–671.
- 909 16. Cho J.H. Kim H.B. Kim H.S. Choi S.B. (2008). Identification and characterization of a
910 rice MCM2 homologue required for DNA replication. *BMB Rep.* 41: 581–586.

911 17. Clough S.J. Bent A.F. (1998). Floral dip: A simplified method for *Agrobacterium*-
912 mediated transformation of *Arabidopsis thaliana*. *Plant J.* 16: 735–743.

913 18. Crowe M.L. et al. (2003). CATMA: A complete *Arabidopsis* GST database. *Nucleic Acids*
914 *Res.* 31: 156–158.

915 19. Davis S.J. Vierstra R.D. (1998). Soluble, highly fluorescent variants of green fluorescent
916 protein (GFP) for use in higher plants. *Plant Mol. Biol.* 36: 521–528.

917 20. del Pozo J.C. Estelle M. (1999). The *Arabidopsis* cullin AtCUL1 is modified by the
918 ubiquitin-related protein RUB1. *Proc. Natl. Acad. Sci. USA* 96: 15342–15347.

919 21. de Lucas M. Davière J.M. Rodríguez-Falcón M. Pontin M. Iglesias-Pedraz J.M.
920 Lorrain S. Fankhauser C. Blázquez M.A. Titarenko E. Prat S. (2008). A molecular framework
921 for light and gibberellin control of cell elongation. *Nature* 451: 480–484.

922 22. Denti S. Fernandez-Sanchez M.E. Rogge L. Bianchi E. (2006). The COP9
923 signalosome regulates Skp2 levels and proliferation of human cells. *J. Biol. Chem.* 281: 32188–
924 32196.

925 23. Dieterle M. Zhou Y.C. Schäfer E. Funk M. Kretsch T. (2001). EID1, an F-box protein
926 involved in phytochrome A-specific light signaling. *Genes Dev.* 15: 939–944.

927 24. Dreher K. Callis J. (2007). Ubiquitin, hormones and biotic stress in plants. *Ann. Bot.*
928 (Lond.) 99: 787–822.

929 25. Etesami P. Callis R. Ellwood S. Stanley J. (1988). Delimitation of essential genes of
930 cassava latent virus DNA 2. *Nucleic Acids Res.* 16: 4811–4829.

931 26. Feng S. Ma L. Wang X. Xie D. Dinesh-Kumar S.P. Wei N. Deng X.W. (2003). The
932 COP9 signalosome interacts physically with SCF COI1 and modulates jasmonate responses.
933 *Plant Cell* 15: 1083–1094.

934 27. Fields S. Song O. (1989). A novel genetic system to detect protein-protein interactions.
935 *Nature* 340: 245–246.

936 28. Figueroa P. Gusmaroli G. Serino G. Habashi J. Ma L. Shen Y. Feng S. Bostick
937 M. Callis J. Hellmann H. Deng X.W. (2005). *Arabidopsis* has two redundant Cullin3 proteins
938 that are essential for embryo development and that interact with RBX1 and BTB proteins to form
939 multisubunit E3 ubiquitin ligase complexes in vivo. *Plant Cell* 17: 1180–1195.

940

941 29. Fukumoto A. Tomoda K. Kubota M. Kato J.Y. Yoneda-Kato N. (2005). Small Jab1-
942 containing subcomplex is regulated in an anchorage- and cell cycle-dependent manner, which is
943 abrogated by ras transformation. *FEBS Lett.* 579: 1047–1054.

944 30. Gagnot S. Tamby J.P. Martin-Magniette M.L. Bitton F. Taconnat L. Balzergue S.
945 Aubourg S. Renou J.P. Lecharny A. Brunaud V. (2008). CATdb: A public access to Arabidopsis
946 transcriptome data from the URGV-CATMA platform. *Nucleic Acids Res.* 36(Database issue):
947 D986–D990.

948 31. Gilkerson J. Hu J. Brown J. Jones A. Sun T.P. Callis J. (2009). Isolation and
949 characterization of cul1-7, a recessive allele of CULLIN1 that disrupts SCF function at the C
950 terminus of CUL1 in Arabidopsis thaliana. *Genetics* 181: 945–963.

951 32. Gouy M. Guindon S. Gascuel O. (2010). SeaView version 4: A multiplatform graphical
952 user interface for sequence alignment and phylogenetic tree building. *Mol. Biol. Evol.* 27: 221–
953 224.

954 33. Gray W.M. del Pozo J.C. Walker L. Hobbie L. Risseeuw E. Banks T. Crosby W.L.
955 Yang M. Ma H. Estelle M. (1999). Identification of an SCF ubiquitin-ligase complex required for
956 auxin response in Arabidopsis thaliana. *Genes Dev.* 13: 1678–1691.

957 34. Gusmaroli G. Feng S. Deng X.W. (2004). The Arabidopsis CSN5A and CSN5B subunits
958 are present in distinct COP9 signalosome complexes, and mutations in their JAMM domains
959 exhibit differential dominant negative effects on development. *Plant Cell* 16: 2984–3001.

960 35. Gusmaroli G. Figueroa P. Serino G. Deng X.W. (2007). Role of the MPN subunits in
961 COP9 signalosome assembly and activity, and their regulatory interaction with Arabidopsis
962 Cullin3-based E3 ligases. *Plant Cell* 19: 564–581.

963 36. Hanley-Bowdoin L. Settlege S.B. Robertson D. (2004). Reprogramming plant gene
964 expression: A prerequisite to geminivirus DNA replication. *Mol. Plant Pathol.* 5: 149–156.

965 37. Hao L. Wang H. Sunter G. Bisaro D.M. (2003). Geminivirus AL2 and L2 proteins
966 interact with and inactivate SNF1 kinase. *Plant Cell* 15: 1034–1048.

967 38. Harmon F.G. Kay S.A. (2003). The F box protein AFR is a positive regulator of
968 phytochrome A-mediated light signaling. *Curr. Biol.* 13: 2091–2096.

969 39. Hartitz M.D. Sunter G. Bisaro D.M. (1999). The tomato golden mosaic virus
970 transactivator (TrAP) is a single-stranded DNA and zinc-binding phosphoprotein with an acidic
971 activation domain. *Virology* 263: 1–14.

972 40. Hellens R.P. Edwards E.A. Leyland N.R. Bean S. Mullineaux P.M. (2000). pGreen:
973 A versatile and flexible binary Ti vector for Agrobacterium-mediated plant transformation. *Plant*
974 *Mol. Biol.* 42: 819–832.

975 41. Hilson P. et al. (2004). Versatile gene-specific sequence tags for Arabidopsis functional
976 genomics: Transcript profiling and reverse genetics applications. *Genome Res.* 14(10B): 2176–
977 2189.

978 42. Ho S.N. Hunt H.D. Horton R.M. Pullen J.K. Pease L.R. (1989). Site-directed
979 mutagenesis by overlap extension using the polymerase chain reaction. *Gene* 77: 51–59.

980 43. Hotton S.K. Callis J. (2008). Regulation of cullin RING ligases. *Annu. Rev. Plant Biol.*
981 59: 467–489.

982 44. Hsieh Y.H. Su I.J. Wang H.C. Tsai J.H. Huang Y.J. Chang W.W. Lai M.D. Lei
983 H.Y. Huang W. (2007). Hepatitis B virus pre-S2 mutant surface antigen induces degradation of
984 cyclin-dependent kinase inhibitor p27Kip1 through c-Jun activation domain-binding protein 1. *Mol.*
985 *Cancer Res.* 5: 1063–1072.

986 45. Hua Z. Zou C. Shiu S.H. Vierstra R.D. (2011). Phylogenetic comparison of F-Box
987 (FBX) gene superfamily within the plant kingdom reveals divergent evolutionary histories
988 indicative of genomic drift. *PLoS ONE* 6: e16219.

989 46. Isaacson M.K. Ploegh H.L. (2009). Ubiquitination, ubiquitin-like modifiers, and
990 deubiquitination in viral infection. *Cell Host Microbe* 5: 559–570.

991 47. James P. Halladay J. Craig E.A. (1996). Genomic libraries and a host strain designed
992 for highly efficient two-hybrid selection in yeast. *Genetics* 144: 1425–1436.

993 48. Kameda K. Fukao M. Kobayashi T. Tsutsuura M. Nagashima M. Yamada Y.
994 Yamashita T. Tohse N. (2006). CSN5/Jab1 inhibits cardiac L-type Ca²⁺ channel activity through
995 protein-protein interactions. *J. Mol. Cell. Cardiol.* 40: 562–569.

996 49. Kandan A. Commare R.R. Nandakumar R. Ramiah M. Raguchander T. Samiyappan
997 R. (2002). Induction of phenylpropanoid metabolism by *Pseudomonas fluorescens* against tomato
998 spotted wilt virus in tomato. *Folia Microbiol. (Praha)* 47: 121–129.

999 50. Kempema L.A. Cui X. Holzer F.M. Walling L.L. (2007). Arabidopsis transcriptome
1000 changes in response to phloem-feeding silverleaf whitefly nymphs. Similarities and distinctions in
1001 responses to aphids. *Plant Physiol.* 143: 849–865.

1002 51. Kertbundit S. De Greve H. Deboeck F. Van Montagu M. Hernalsteens J.P. (1991).
1003 In vivo random beta-glucuronidase gene fusions in *Arabidopsis thaliana*. Proc. Natl. Acad. Sci.
1004 USA 88: 5212–5216.

1005 52. Komatsu K. Hashimoto M. Ozeki J. Yamaji Y. Maejima K. Senshu H. Himeno M.
1006 Okano Y. Kagiwada S. Namba S. (2010). Viral-induced systemic necrosis in plants involves
1007 both programmed cell death and the inhibition of viral multiplication, which are regulated by
1008 independent pathways. Mol. Plant Microbe Interact. 23: 283–293.

1009 53. Kovac M. Müller A. Milanovic Jarh D. Milavec M. Düchting P. Ravnikar M. (2009).
1010 Multiple hormone analysis indicates involvement of jasmonate signalling in the early defence of
1011 potato to potato virus YNTN. Biol. Plant 53: 195–199.

1012 54. Kuroda H. Takahashi N. Shimada H. Seki M. Shinozaki K. Matsui M. (2002).
1013 Classification and expression analysis of *Arabidopsis* F-box-containing protein genes. Plant Cell
1014 Physiol. 43: 1073–1085.

1015 55. Kwok S.F. Solano R. Tsuge T. Chamovitz D.A. Ecker J.R. Matsui M. Deng X.W.
1016 (1998). *Arabidopsis* homologs of a c-Jun coactivator are present both in monomeric form and in
1017 the COP9 complex, and their abundance is differentially affected by the pleiotropic *cop/det/fus*
1018 mutations. Plant Cell 10: 1779–1790.

1019 56. Lageix S. Catrice O. Deragon J.M. Gronenborn B. Péliissier T. Ramírez B.C. (2007).
1020 The nanovirus-encoded Clink protein affects plant cell cycle regulation through interaction with
1021 the retinoblastoma-related protein. J. Virol. 81: 4177–4185.

1022 57. Liu Y. Schiff M. Dinesh-Kumar S.P. (2004). Involvement of MEK1 MAPKK, NTF6 MAPK,
1023 WRKY/MYB transcription factors, COI1 and CTR1 in N-mediated resistance to tobacco mosaic
1024 virus. Plant J. 38: 800–809.

1025 58. Liu Y. Schiff M. Serino G. Deng X.W. Dinesh-Kumar S.P. (2002). Role of SCF
1026 ubiquitin-ligase and the COP9 signalosome in the N gene-mediated resistance response to
1027 Tobacco mosaic virus. Plant Cell 14: 1483–1496.

1028 59. Lurin C. et al. (2004). Genome-wide analysis of *Arabidopsis* pentatricopeptide repeat
1029 proteins reveals their essential role in organelle biogenesis. Plant Cell 16: 2089–2103.

1030 60. Lyapina S. Cope G. Shevchenko A. Serino G. Tsuge T. Zhou C. Wolf D.A. Wei
1031 N. Shevchenko A. Deshaies R.J. (2001). Promotion of NEDD-CUL1 conjugate cleavage by
1032 COP9 signalosome. Science 292: 1382–1385.

1033 61. Mahalingam S. Ayyavoo V. Patel M. Kieber-Emmons T. Kao G.D. Muschel R.J.
1034 Weiner D.B. (1998). HIV-1 Vpr interacts with a human 34-kDa mov34 homologue, a cellular factor
1035 linked to the G2/M phase transition of the mammalian cell cycle. *Proc. Natl. Acad. Sci. USA* 95:
1036 3419–3424.

1037 62. Marrocco K. Zhou Y. Bury E. Dieterle M. Funk M. Genschik P. Krenz M. Stolpe
1038 T. Kretsch T. (2006). Functional analysis of EID1, an F-box protein involved in phytochrome A-
1039 dependent light signal transduction. *Plant J.* 45: 423–438.

1040 63. Matros A. Mock H.P. (2004). Ectopic expression of a UDP-glucose:phenylpropanoid
1041 glucosyltransferase leads to increased resistance of transgenic tobacco plants against infection
1042 with Potato Virus Y. *Plant Cell Physiol.* 45: 1185–1193.

1043 64. Moon J. Zhao Y. Dai X. Zhang W. Gray W.M. Huq E. Estelle M. (2007). A new
1044 CULLIN 1 mutant has altered responses to hormones and light in *Arabidopsis*. *Plant Physiol.* 143:
1045 684–696.

1046 65. Morilla G. Castillo A.G. Preiss W. Jeske H. Bejarano E.R. (2006). A versatile
1047 transreplication-based system to identify cellular proteins involved in geminivirus replication. *J.*
1048 *Virology*. 80: 3624–3633.

1049 66. Mundt K.E. Liu C. Carr A.M. (2002). Deletion mutants in COP9/signalosome subunits
1050 in fission yeast *Schizosaccharomyces pombe* display distinct phenotypes. *Mol. Biol. Cell* 13:
1051 493–502.

1052 67. Murray S.L. Thomson C. Chini A. Read N.D. Loake G.J. (2002). Characterization of
1053 a novel, defense-related *Arabidopsis* mutant, *cir1*, isolated by luciferase imaging. *Mol. Plant*
1054 *Microbe Interact.* 15: 557–566.

1055 68. Nemhauser J.L. Hong F. Chory J. (2006). Different plant hormones regulate similar
1056 processes through largely nonoverlapping transcriptional responses. *Cell* 126: 467–475.

1057 69. Nordgård O. Dahle O. Andersen T.O. Gabrielsen O.S. (2001). JAB1/CSN5 interacts
1058 with the GAL4 DNA binding domain: A note of caution about two-hybrid interactions. *Biochimie*
1059 83: 969–971.

1060 70. Oh W. Yang M.R. Lee E.W. Park K.M. Pyo S. Yang J.S. Lee H.W. Song J. (2006).
1061 Jab1 mediates cytoplasmic localization and degradation of West Nile virus capsid protein. *J. Biol.*
1062 *Chem.* 281: 30166–30174.

1063 71. Oron E. Mannervik M. Rencus S. Harari-Steinberg O. Neuman-Silberberg S. Segal
1064 D. Chamovitz D.A. (2002). COP9 signalosome subunits 4 and 5 regulate multiple pleiotropic
1065 pathways in *Drosophila melanogaster*. *Development* 129: 4399–4409.

1066 72. Panchuk I.I. Volkov R.A. Schöffl F. (2002). Heat stress- and heat shock transcription
1067 factor-dependent expression and activity of ascorbate peroxidase in *Arabidopsis*. *Plant Physiol.*
1068 129: 838–853.

1069 73. Raja P. Wolf J.N. Bisaro D.M. (2010). RNA silencing directed against geminiviruses:
1070 Post-transcriptional and epigenetic components. *Biochim. Biophys. Acta* 1799: 337–351.

1071 74. Ren C. Pan J. Peng W. Genschik P. Hobbie L. Hellmann H. Estelle M. Gao B.
1072 Peng J. Sun C. Xie D. (2005). Point mutations in *Arabidopsis* Cullin1 reveal its essential role in
1073 jasmonate response. *Plant J.* 42: 514–524.

1074 75. Rojas M.R. Hagen C. Lucas W.J. Gilbertson R.L. (2005). Exploiting chinks in the
1075 plant's armor: Evolution and emergence of geminiviruses. *Annu. Rev. Phytopathol.* 43: 361–394.

1076 76. Sambrook J. Russell D.W. (2001). *Molecular Cloning: A Laboratory Manual*. (Cold
1077 Spring Harbor, NY: Cold Spring Harbor Laboratory Press).

1078 77. Santner A. Estelle M. (2009). Recent advances and emerging trends in plant hormone
1079 signalling. *Nature* 459: 1071–1078.

1080 78. Schwechheimer C. Serino G. Callis J. Crosby W.L. Lyapina S. Deshaies R.J. Gray
1081 W.M. Estelle M. Deng X.W. (2001). Interactions of the COP9 signalosome with the E3 ubiquitin
1082 ligase SCFTIR1 in mediating auxin response. *Science* 292: 1379–1382.

1083 79. Schwechheimer C. Serino G. Deng X.W. (2002). Multiple ubiquitin ligase-mediated
1084 processes require COP9 signalosome and AXR1 function. *Plant Cell* 14: 2553–2563.

1085 80. Sharma P. Ikegami M. Kon T. (2010). Identification of the virulence factors and
1086 suppressors of posttranscriptional gene silencing encoded by *Ageratum* yellow vein virus, a
1087 monopartite begomovirus. *Virus Res.* 149: 19–27.

1088 81. Sheard L.B. et al. (2010). Jasmonate perception by inositol-phosphate-potentiated
1089 COI1-JAZ co-receptor. *Nature* 468: 400–405.

1090 82. Stenzel I. Hause B. Maucher H. Pitzschke A. Miersch O. Ziegler J. Ryan C.A.
1091 Wasternack C. (2003). Allene oxide cyclase dependence of the wound response and vascular
1092 bundle-specific generation of jasmonates in tomato - Amplification in wound signalling. *Plant J.*
1093 33: 577–589.

1094 83. Stuttmann J. Lechner E. Guérois R. Parker J.E. Nussaume L. Genschik P. Noël
1095 L.D. (2009). COP9 signalosome- and 26S proteasome-dependent regulation of SCFTIR1
1096 accumulation in Arabidopsis. *J. Biol. Chem.* 284: 7920–7930.

1097 84. Sunter G. Bisaro D.M. (1992). Transactivation of geminivirus AR1 and BR1 gene
1098 expression by the viral AL2 gene product occurs at the level of transcription. *Plant Cell* 4: 1321–
1099 1331.

1100 85. Sunter G. Sunter J.L. Bisaro D.M. (2001). Plants expressing tomato golden mosaic
1101 virus AL2 or beet curly top virus L2 transgenes show enhanced susceptibility to infection by DNA
1102 and RNA viruses. *Virology* 285: 59–70.

1103 86. Tanaka Y. et al. (2006). The hepatitis B virus X protein enhances AP-1 activation through
1104 interaction with Jab1. *Oncogene* 25: 633–642.

1105 87. Tanguy G. Drévilion L. Arous N. Hasnain A. Hinzpeter A. Fritsch J. Goossens M.
1106 Fanen P. (2008). CSN5 binds to misfolded CFTR and promotes its degradation. *Biochim. Biophys.*
1107 *Acta* 1783: 1189–1199.

1108 88. Thines B. Katsir L. Melotto M. Niu Y. Mandaokar A. Liu G. Nomura K. He S.Y.
1109 Howe G.A. Browse J. (2007). JAZ repressor proteins are targets of the SCF(COI1) complex
1110 during jasmonate signalling. *Nature* 448: 661–665.

1111 89. Tomoda K. Kato J.Y. Tatsumi E. Takahashi T. Matsuo Y. Yoneda-Kato N. (2005).
1112 The Jab1/COP9 signalosome subcomplex is a downstream mediator of Bcr-Abl kinase activity
1113 and facilitates cell-cycle progression. *Blood* 105: 775–783.

1114 90. Trinks D. Rajeswaran R. Shivaprasad P.V. Akbergenov R. Oakeley E.J. Veluthambi
1115 K. Hohn T. Pooggin M.M. (2005). Suppression of RNA silencing by a geminivirus nuclear
1116 protein, AC2, correlates with transactivation of host genes. *J. Virol.* 79: 2517–2527.

1117 91. Valenzuela-Soto J.H. Estrada-Hernández M.G. Ibarra-Laclette E. Délano-Frier J.P.
1118 (2010). Inoculation of tomato plants (*Solanum lycopersicum*) with growth-promoting *Bacillus*
1119 *subtilis* retards whitefly *Bemisia tabaci* development. *Planta* 231: 397–410.

1120 92. van den Burg H.A. Tsitsigiannis D.I. Rowland O. Lo J. Rallapalli G. Maclean D.
1121 Takken F.L. Jones J.D. (2008). The F-box protein ACRE189/ACIF1 regulates cell death and
1122 defense responses activated during pathogen recognition in tobacco and tomato. *Plant Cell* 20:
1123 697–719.

1124 93. van Engelen F.A. Molthoff J.W. Conner A.J. Nap J.P. Pereira A. Stiekema W.J.
1125 (1995). pBINPLUS: an improved plant transformation vector based on pBIN19. *Transgenic Res.*
1126 4: 288–290.

1127 94. van Wezel R. Liu H. Tien P. Stanley J. Hong Y. (2001). Gene C2 of the monopartite
1128 geminivirus tomato yellow leaf curl virus-China encodes a pathogenicity determinant that is
1129 localized in the nucleus. *Mol. Plant Microbe Interact.* 14: 1125–1128.

1130 95. Vierstra R.D. (2009). The ubiquitin-26S proteasome system at the nexus of plant biology.
1131 *Nat. Rev. Mol. Cell Biol.* 10: 385–397.

1132 96. Vigliocco A. Bonamico B. Alemano S. Miersch O. Abdala G. (2002). Stimulation of
1133 jasmonic acid production in *Zea mays* L. infected by the maize rough dwarf virus-Río Cuarto.
1134 Reversion of symptoms by salicylic acid. *Biocell* 26: 369–374.

1135 97. Voinnet O. Rivas S. Mestre P. Baulcombe D. (2003). An enhanced transient
1136 expression system in plants based on suppression of gene silencing by the p19 protein of tomato
1137 bushy stunt virus. *Plant J.* 33: 949–956.

1138 98. Wang X. Feng S. Nakayama N. Crosby W.L. Irish V. Deng X.W. Wei N. (2003).
1139 The COP9 signalosome interacts with SCF UFO and participates in Arabidopsis flower
1140 development. *Plant Cell* 15: 1071–1082.

1141 99. Wang X. Kang D. Feng S. Serino G. Schwechheimer C. Wei N. (2002). CSN1 N-
1142 terminal-dependent activity is required for Arabidopsis development but not for Rub1/Nedd8
1143 deconjugation of cullins: A structure-function study of CSN1 subunit of COP9 signalosome. *Mol.*
1144 *Biol. Cell* 13: 646–655.

1145 100. Wartig L. Kheyr-Pour A. Noris E. De Kouchkovsky F. Jouanneau F. Gronenborn B.
1146 Jupin I. (1997). Genetic analysis of the monopartite tomato yellow leaf curl geminivirus: roles of
1147 V1, V2, and C2 ORFs in viral pathogenesis. *Virology* 228: 132–140.

1148 101. Wei N. Serino G. Deng X.W. (2008). The COP9 signalosome: More than a protease.
1149 *Trends Biochem. Sci.* 33: 592–600.

1150 102. Yang J.Y. Iwasaki M. Machida C. Machida Y. Zhou X. Chua N.H. (2008). betaC1,
1151 the pathogenicity factor of TYLCCNV, interacts with AS1 to alter leaf development and suppress
1152 selective jasmonic acid responses. *Genes Dev.* 22: 2564–2577.

1153 103. Yang Y.H. Speed T. (2002). Design issues for cDNA microarray experiments. *Nat. Rev.*
1154 *Genet.* 3: 579–588.

1155 104. Zhang Y. Xu W. Li Z. Deng X.W. Wu W. Xue Y. (2008). F-box protein DOR functions
1156 as a novel inhibitory factor for abscisic acid-induced stomatal closure under drought stress in
1157 Arabidopsis. *Plant Physiol.* 148: 2121–2133.

1158

1159 **FIGURE LEGENDS**

1160 **Figure 1.** In Vivo Interaction between Geminivirus C2 and the Plant CSN5. (A) BiFC analyses
1161 showing interaction between geminivirus C2/L2 (C2-TS stands for TYLCSV C2; C2-TM stands
1162 for TYLCV C2; L2-BC stands for BCTV L2) and the plant CSN5 (CSN5 stands for Arabidopsis
1163 CSN5A; SICSN5 stands for *S. lycopersicum* cultivar Moneymaker CSN5). GUS stands for *A.*
1164 *thaliana* β -glucuronidase, used as a negative control. *N. benthamiana* leaves coinfiltrated with
1165 constructs expressing C2/L2, CSN5, or β -glucuronidase fused to the YFP C terminus (CYFP) or
1166 N terminus (NYFP) were observed under the confocal microscope 3 d after infiltration. Leaves
1167 were infiltrated with a 4 μ g/mL DAPI solution 3 d after infiltration and observed under the confocal
1168 microscope 0.5 to 5 h later. No differences were observed between the two pair-wise
1169 combinations; only one of the combinations is shown.

1170 (B) Subcellular localization of GFP-C2-TS fusion protein in epidermal cells of *N. benthamiana*. *N.*
1171 *benthamiana* leaves infiltrated with a construct expressing a GFP-C2-TS fusion protein were
1172 infiltrated with a 4 μ g/mL DAPI solution 3 d after infiltration and observed under the confocal
1173 microscope 0.5 to 5 h later. GFP-C2-TS is mainly localized into the nucleus. GFP fluorescence,
1174 DAPI staining, and merge, including bright-field channel, are shown.

1175 **Figure 2.** Immunoblot Analysis of 2-Week-Old Wild-Type, *csn5a*, and Kanamycin-Resistant
1176 Transgenic C2-TS, C2-TM, and L2-BC Arabidopsis Seedlings.

1177 (A) Detection of Arabidopsis CUL1, CUL3, and CUL4. Total proteins were subjected to SDS-
1178 PAGE and immunoblot analysis with α -CUL1, α -CUL3, and α -CUL4. Equal protein loads were
1179 confirmed using α -RPN6 (RPN6 is a non-ATPase regulatory subunit of the 26S proteasome).
1180 Rubylated (Rub-CUL) and derubylated Cullins (CUL) are indicated by arrows. WT, wild type.

1181 (B) to (D) Immunoblot analyses of Superose 6 gel filtration fractions. Column fractions were
1182 subjected to SDS-PAGE and immunoblotted with α -CSN5 (B), α -CUL1 (C), α -RBX1, or α -ASK1
1183 (D). Fraction numbers are indicated. Lane T contains the total unfractionated extracts.

1184 **Figure 3.** Root and Hypocotyl Length Analysis of C2/L2 Transgenic Plants.

1185 (A) Total root length of transgenic C2-TS, C2-TM, and L2-BC or wild-type Arabidopsis seedlings
1186 (WT) was measured every 24 h beginning 4 d after germination ($n \geq 14$). Bars represent se.

1187 (B) Hypocotyl length of 9-d-old dark-grown transgenic C2-TS, C2-TM, and L2-BC or wild-type
1188 Arabidopsis seedlings. Bars represent sd. Asterisks indicate a statistically significant difference
1189 when compared with the wild-type value according to Mann-Whitney rank sum test. $n \geq 30$; the
1190 experiment was repeated three times.

1191 **Figure 4.** Reduced Auxin, Jasmonate, and Gibberellin Response and Enhanced Ethylene
1192 Response in Transgenic C2/L2 Arabidopsis Lines.

1193 Hormone sensitivity was measured as root growth inhibition. Experiments were repeated at least
1194 three times independently; results from one of the replicates are represented ($n \geq 15$). Five-day-
1195 old seedlings were grown on exogenous hormone for an additional 5 d. Bars represent se.
1196 Asterisks indicate a statistically significant difference when compared with the wild-type value
1197 according to Mann-Whitney rank sum test. WT, wild type.

1198 **Figure 5.** Expression Level of Hormone-Responsive Genes in C2/L2 Transgenic Plants.

1199 Relative expression level of marker genes of the ethylene (ERF1 and ERS2), auxin (PIN1 and
1200 IAA19), gibberellin (MFC19.13 and MHJ24.10), and jasmonate (OPR3 and JR1) response in
1201 mock- or hormone-treated transgenic C2-TS, C2-TM, and L2-BC and control Arabidopsis
1202 seedlings determined by quantitative real-time PCR. C2/L2-expressing lines are compared with
1203 the control in each condition. Actin was used as the internal control.

1204 **Figure 6.** Drought-Related Phenotypes of Transgenic C2-TS, C2-TM, and L2-BC and Wild-Type
1205 Arabidopsis Plants.

1206 (A) Phenotype of 7-week-old plants after 10 d without water supply. WT, wild type.

1207 (B) Weight loss in detached leaves. Rosette leaves from 4-week-old plants were detached, placed
1208 on weighing dishes, and allowed to dry at room conditions. Weight of the samples was recorded
1209 at 0.5, 1, 2, 3, and 4 h. $n = 5$; bars represent se.

1210 (C) Stomata in epidermal peels after inducing stomatal aperture and treating with 5 μ M ABA or
1211 mock solution for 1 h.

1212 **Figure 7.** In Vivo Degradation Assay of YFP-GAI Fusion Protein.

1213 (A) The construct expressing YFP-GAI was agroinfiltrated in *N. benthamiana* leaves alone (control)
1214 or coinfiltrated with constructs expressing C2-TS, C2-TM, or L2-BC. Three days after infiltration,
1215 agroinfiltrated leaves were sprayed with 100 μ M GA3 or mock solution and visualized under the
1216 epifluorescence microscope 1 to 2 h later.

1217 (B) Detection of YFP-GAI or GFP (as a control) in *N. benthamiana* leaves agroinfiltrated with the
1218 construct expressing YFP-GAI alone or together with constructs expressing C2-TS, C2-TM, and
1219 L2- BC and treated with 100 μ M GA3 or mock solution. Total proteins were subjected to SDS-
1220 PAGE and immunoblot analysis with α -GFP, which also recognizes YFP. Coomassie blue staining
1221 of the protein blot is shown as loading control.

1222 (D) Stomatal aperture in epidermal peels after treatment with 5 μ M ABA or mock solution. The
1223 experiments were repeated three times independently; at least 30 stomatal apertures were
1224 measured in each condition. Bars represent sd.

1225 **Figure 8.** Venn Diagrams Depicting the Intersection between Upregulated or Downregulated
1226 Genes in C2-TS Transgenic Plants or MeJA-Treated Col-0 Plants (Nemhauser et al., 2006).

1227 The number of genes in each category is indicated. Numbers of genes higher than those expected
1228 in a random distribution, with $\alpha = 0.05$, are underlined. The significance of matches being higher
1229 than explained by random sampling was tested by assuming a Poisson distribution from a mean
1230 value calculated as $\mu = G1 \times (G2/Gt)$, since any gene in G1 has a G2/Gt possibility to belong to
1231 G2, and being G1 and G2 the subsets of genes to be compared and Gt the total number of genes
1232 represented in the microarray. An asterisk by the number of genes in an intersection indicates
1233 that there are overrepresented GO terms in that subset of genes (Table 2).

1234 **Figure 9.** BCTV Infection of Arabidopsis Plants Treated with MeJA or Mock Solution.

1235 Four- to five-week-old Arabidopsis plants were agroinoculated with BCTV, treated every other
1236 day with MeJA or mock solution (12 plants per treatment), and scored for the appearance of
1237 symptoms at 28 DAI. Total DNA was extracted from each plant independently and subjected to
1238 DNA gel blot to quantify viral DNA accumulation. The experiment was repeated twice; no
1239 differences in symptom development or viral DNA accumulation were observed between the
1240 replicates. The results of one of the experiments are shown.

1241

1242 (A) Symptom severity at 28 DAI according to the severity index described in Baliji et al. (2007),
 1243 where 0 represent symptomless plants and 1 to 4 represent plants showing increasing symptom
 1244 severity.

1245 (B) Relative viral DNA accumulation. Bars represent se.

1246

1247 **Table 1.** Summary of the symptoms caused by geminiviral proteins C2, C4, and V2 expressed
 1248 from *Potato virus X* (PVX) at 16 days post infection(a)

Table 1. Summary of the symptoms caused by geminiviral proteins C2, C4, and V2 expressed from *Potato virus X* (PVX) at 16 days post infection

Protein	TYLCSV	TYLVC	TYLCV-Mld	TYLC-MaIV	PVX	NSs
Local						
C2	N	Y	Y	Y	Y	N
C4	Y	Y	Y	Y	Y	N
V2	N	N	N	N	Y	N
Systemic						
C2	N	C	C	C+	C	N
C4	C+	C+	C+	C	C	N
V2	N	N	N	N	C	N

1249

1250 (a) Viral open reading frames were expressed from a PVX vector and tested individually in 16c
 1251 *Nicotiana benthamiana* leaves co-infiltrated with a 35S-green fluorescent protein (GFP)-
 1252 expressing *Agrobacterium tumefaciens* culture. Co-agroinoculation of 35S-GFP with either the
 1253 empty PVX vector (PVX) or a recombinant PVX virus expressing a gene-silencing suppressor
 1254 from *Tomato spotted wilt virus*, the nonstructural protein (NSs), were used as negative and
 1255 positive controls, respectively. Local symptoms: yellowing (Y) or a necrosis (N) of the
 1256 agroinfiltrated area. Systemic symptoms: mild symptoms typical of a PVX infection, including mild
 1257 vein yellowing, very mild vein thickening and a faint mosaic (C), enhanced PVX symptoms (C+),
 1258 or systemic necrosis(N). Viruses: *Tomato yellow leaf curl Sardinia virus* (TYLCSV), *Tomato yellow*
 1259 *leaf curl virus* (TYLCV), TYLCV-mild (Mld), and *Tomato yellow leaf curl Malaga virus* (TYLCMaIV).

1260

1261 **Table 1.** Open in new tabInteraction between Geminivirus C2 and the Plant CSN5 in Yeast

Bait	Prey	Interaction
C2 ₁₋₇₈ -TS	CSN5A ₄₄₋₃₅₇	Yes

Bait	Prey	Interaction
C2 ₁₋₇₈ -TM	CSN5A ₄₄₋₃₅₇	Yes
L2 ₁₋₁₀₈ -BC	CSN5A ₄₄₋₃₅₇	Yes
P53	CSN5A ₄₄₋₃₅₇	No
C2 ₁₋₇₈ -TS	CSN5B ₄₄₋₃₅₈	Yes
C2 ₁₋₇₈ -TM	CSN5B ₄₄₋₃₅₈	Yes
L2 ₁₋₁₀₈ -BC	CSN5B ₄₄₋₃₅₈	Yes
P53	CSN5B ₄₄₋₃₅₈	No
C2 ₁₋₇₈ -TS	SICSN5 ₅₇₋₃₆₇	Yes
C2 ₁₋₇₈ -TM	SICSN5 ₅₇₋₃₆₇	Yes
L2 ₁₋₁₀₈ -BC	SICSN5 ₅₇₋₃₆₇	Yes
P53	SICSN5 ₅₇₋₃₆₇	No
C2 ₁₋₇₈ -TS	AgT	No
C2 ₁₋₇₈ -TM	AgT	No
L2 ₁₋₁₀₈ -BC	AgT	No

1262 C2-TS stands for TYLCSV C2; C2-TM stands for TYLCV C2; L2-BC stands for BCTV L2.
 1263 CSN5A and CSN5B are from *Arabidopsis*; SICSN5 is CSN5 from tomato cultivar Moneymaker.
 1264 Interaction was indicated by the ability of cells to grow on medium lacking His and Ade and
 1265 containing 50 mM 3-aminotriazole. P53 stands for the murine p53 protein fused to the GAL4
 1266 DBD (pGBKT7-53; Clontech), and AgT stands for the SV40 large T antigen fused to the GAL4
 1267 AD fused to the GAL4 (pGADT7-T; Clontech); both are used as negative controls.

1268

1269 **Table 2.** Open in new tab Gene Ontology Analysis of Differentially Expressed Genes

Nonredundant GO Categories	GO	Level	Differentially Expressed (%)	Expected Frequency	P Value
Downregulated Genes					
Response to stress	to	3	16.7% (107)	5.5%	8.98e-20
Secondary metabolic process		3	6.7% (43)	1.3%	1.84e-15
Immune response		3	3.3% (21)	0.6%	5.27e-07
Catabolic process		3	6.2% (40)	2.2%	9.73e-06
Defense response		3	5.5% (35)	1.9%	8.21e-05

Nonredundant GO Categories	Level	Differentially Expressed (%)	Expected Frequency	P Value
Nitrogen compound metabolic process	3	4.7% (30)	1.6%	0.00041
Cellular biosynthetic process	4	13.2% (85)	4.8%	9.45e-13
Organic acid metabolic process	4	7.3% (47)	2.2%	7.80e-09
Aromatic compound metabolic process	4	4.5% (29)	1.0%	1.32e-08
Response to wounding	4	2.8% (18)	0.4%	2.05e-07
Innate immune response	4	3.1% (20)	0.6%	6.74e-07
Heterocycle metabolic process	4	3.1% (20)	0.7%	1.89e-05
Pigment metabolic process	4	2.3% (15)	0.4%	2.04e-05

Nonredundant GO Categories	GO	Level	Differentially Expressed (%)	Expected Frequency	P Value
Cellular process	catabolic	4	5.9% (38)	2.1%	2.59e-05
Amine process	metabolic	4	4.7% (30)	1.4%	3.01e-05
Response to water		4	2.5% (16)	0.5%	0.00010
Response to jasmonic acid stimulus	to acid	4	2.5% (16)	0.5%	0.00031
Sulfur process	metabolic	4	1.9% (12)	0.3%	0.00167
Carboxylic acid metabolic process	acid	5	7.3% (47)	2.2%	7.27e-09
Aromatic compound biosynthetic process		5	3.3% (21)	0.6%	1.92e-07
Response to heat		5	2.5% (16)	0.4%	7.85e-06

Nonredundant GO Categories	GO	Level	Differentially Expressed (%)	Expected Frequency	P Value
Nitrogen compound biosynthetic process		5	3.0% (19)	0.6%	2.71e-05
Response to water deprivation		5	2.5% (16)	0.5%	4.14e-05
Response to oxidative stress	to	5	3.3% (21)	0.8%	5.57e-05
Response to cold		5	2.8% (18)	0.7%	0.00129
Amino acid derivative biosynthetic process	acid	6	3.6% (23)	0.6%	5.91e-09
Defense response, incompatible interaction		6	2.6% (17)	0.3%	5.64e-08
Cellular carbohydrate metabolic process		6	4.2% (27)	1.2%	4.32e-05

Nonredundant Categories	GO	Level	Differentially Expressed (%)	Expected Frequency	P Value
Response to desiccation	to	6	1.1% (7)	0.1%	9.12e-05
Amino acid metabolic process	acid	6	4.0% (26)	1.2%	9.23e-05
Biogenic amine metabolic process	amine	6	1.4% (9)	0.2%	0.00025
Toxin catabolic process	catabolic	6	1.1% (7)	0.1%	0.00398
Porphyrin catabolic process		6	0.8% (5)	0.0%	0.00412
Jasmonic acid and ethylene-dependent systemic resistance		7	1.2% (8)	0.1%	0.00010
Indole derivative biosynthetic process	derivative	7	1.2% (8)	0.1%	0.00010
Phenylpropanoid biosynthetic process		7	2.2% (14)	0.4%	0.00015

Nonredundant GO Categories	Level	Differentially Expressed (%)	Expected Frequency	P Value
Amino acid biosynthetic process	7	2.5% (16)	0.5%	0.00017
Biogenic amine biosynthetic process	7	1.2% (8)	0.1%	0.00076
Indolalkylamine metabolic process	7	0.9% (6)	0.1%	0.00439
Flavonoid biosynthetic process	8	1.6% (10)	0.2%	0.00029
Indoleacetic acid biosynthetic process	8	0.8% (5)	0.0%	0.00054
Tryptophan metabolic process	8	0.9% (6)	0.1%	0.00439
Glycosinolate biosynthetic process	9	1.1% (7)	0.1%	2.89e-05
Jasmonic acid metabolic process	9	1.1% (7)	0.1%	5.27e-05
Oxylipin biosynthetic process	9	1.1% (7)	0.1%	5.27e-05

Nonredundant GO Categories	GO	Level	Differentially Expressed (%)	Expected Frequency	P Value
Upregulated genes					
Response to hormone stimulus	to	3	5.6% (34)	2.4%	0.00738

1270 Nonredundant GO categories identified as enriched among down- or upregulated genes in
1271 C2-TS expressing *Arabidopsis* plants versus control plants. GO category levels are indicated.
1272 The percentages of genes belonging to each category are reported for the differentially
1273 expressed genes and for the genes present in the microarray. The absolute number of
1274 differentially expressed genes belonging to each category is reported in parentheses.

1275
1276 **Table 3.** GO Analysis of the Intersection between C2 Downregulated or Upregulated Genes
1277 and the Upregulated Genes in the MeJA Microarray from Nemhauser et al. (2006)

Downregulated Genes		Level	Differentially Expressed (%)	Expected Frequency	P Value
Nonredundant GO Categories					
Response to stress	to	3	22.8% (26)	5.5%	5.04e-08
Secondary metabolic process		3	8.8% (10)	1.3%	0.00024

Downregulated Genes	Level	Differentially Expressed (%)	Expected Frequency	P Value
Immune response	3	6.1% (7)	0.7%	0.00140
Catabolic process	3	3.5% (4)	0.2%	0.00383
Defense response	3	5.3% (6)	0.5%	0.00160
Nitrogen compound metabolic process	3	9.6% (11)	1.5%	0.00011
Cellular biosynthetic process	4	19.3% (22)	7.3%	0.00263
Organic acid metabolic process	4	18.4% (21)	2.1%	4.07e-12
Aromatic compound metabolic process	4	9.6% (11)	1.0%	1.36e-06
Response to wounding	4	9.6% (11)	0.4%	6.46e-11
Innate immune response	4	6.1% (7)	0.7%	0.00140

Downregulated Genes	Level	Differentially Expressed (%)	Expected Frequency	P Value
Heterocycle metabolic process	4	7.9% (9)	0.6%	4.53e-06
Amine metabolic process	4	5.3% (6)	0.1%	1.64e-06
Response to jasmonic acid stimulus	4	10.5% (12)	0.5%	3.64e-11
Carboxylic acid metabolic process	5	18.4% (21)	2.1%	3.94e-12
Aromatic compound biosynthetic process	5	5.3% (6)	0.6%	0.00577
Nitrogen compound Biosynthetic process	5	7.9% (9)	0.6%	2.49e-06
Amino acid derivative biosynthetic process	6	5.3% (6)	0.6%	0.00702
Defense response,	6	5.3% (6)	0.5%	0.00160

Downregulated Genes	Level	Differentially Expressed (%)	Expected Frequency	P Value
incompatible interaction				
Amino acid metabolic process	6	8.8% (10)	1.1%	5.29e-05
Biogenic amine metabolic process	6	5.3% (6)	0.1%	1.64e-06
Toxin catabolic process	6	3.5% (4)	0.2%	0.00383
Jasmonic acid and ethylene-dependent systemic resistance	7	5.3% (6)	0.1%	2.38e-07
Indole derivative biosynthetic process	7	5.3% (6)	0.1%	3.56e-07
Amino acid biosynthetic process	7	7.0% (8)	0.5%	7.10e-06
Biogenic amine biosynthetic process	7	4.4% (5)	0.1%	3.67e-05

Downregulated Genes	Level	Differentially Expressed (%)	Expected Frequency	P Value
Indolalkylamine metabolic process	7	4.4% (5)	0.1%	3.72e-06
Indoleacetic acid biosynthetic process	8	2.6% (3)	0.0%	0.00035
Trp metabolic process	8	4.4% (5)	0.1%	3.72e-06
Glycosinolate biosynthetic process	9	2.6% (3)	0.1%	0.00930
Jasmonic acid metabolic process	9	5.6% (3)	0.1%	2.48e-08
Oxylipin biosynthetic process	9	5.6% (3)	0.1%	3.35e-08

1278 GO category levels are indicated. The percentages of genes belonging to each category are
1279 reported for the differentially expressed genes and for the genes present in the microarray.
1280 The absolute number of differentially expressed genes belonging to each category is reported
1281 in parentheses.

1282

1283

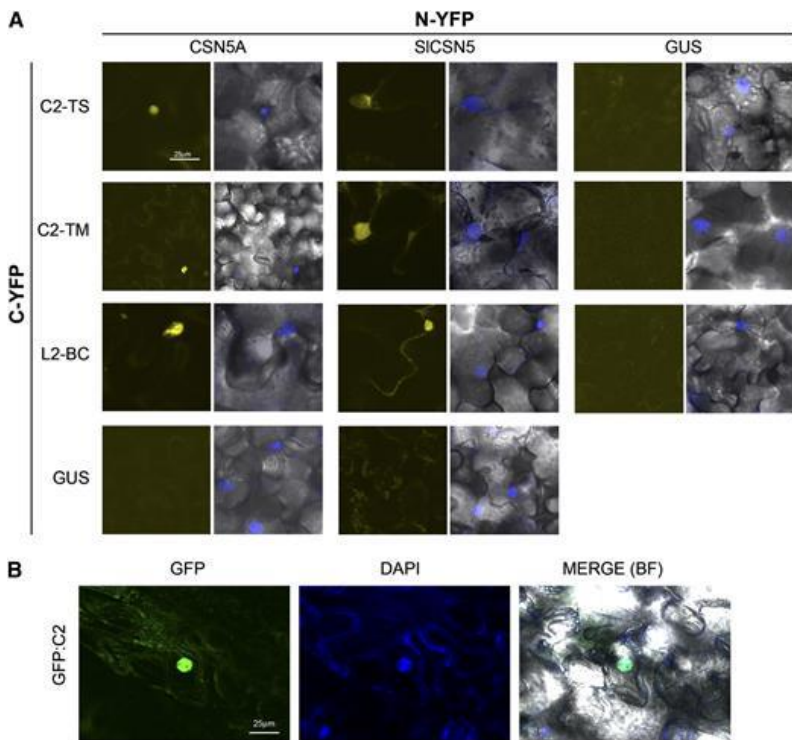
1284

1285

1286 (a) Viruses: *Potato virus X* (PVX), *Tomato yellow leaf curl Sardinia virus* (TYLCSV), *Tomato*
 1287 *yellow leaf curl virus* (TYLCV), TYLCV-mild (Mld), and *Tomato yellow leaf curl Malaga virus*
 1288 (TYLCMaIV). Yes = the viral protein suppressed RNA silencing in this assay; No = the viral
 1289 protein did not suppress RNA silencing in this assay; nd = not determined; Delay = the viral
 1290 protein did not suppress silencing but produced a delay in the process; and * = the viral protein
 1291 produced necrosis and death of the agroinfiltrated plant.

1292

1293 Fig.1



1294

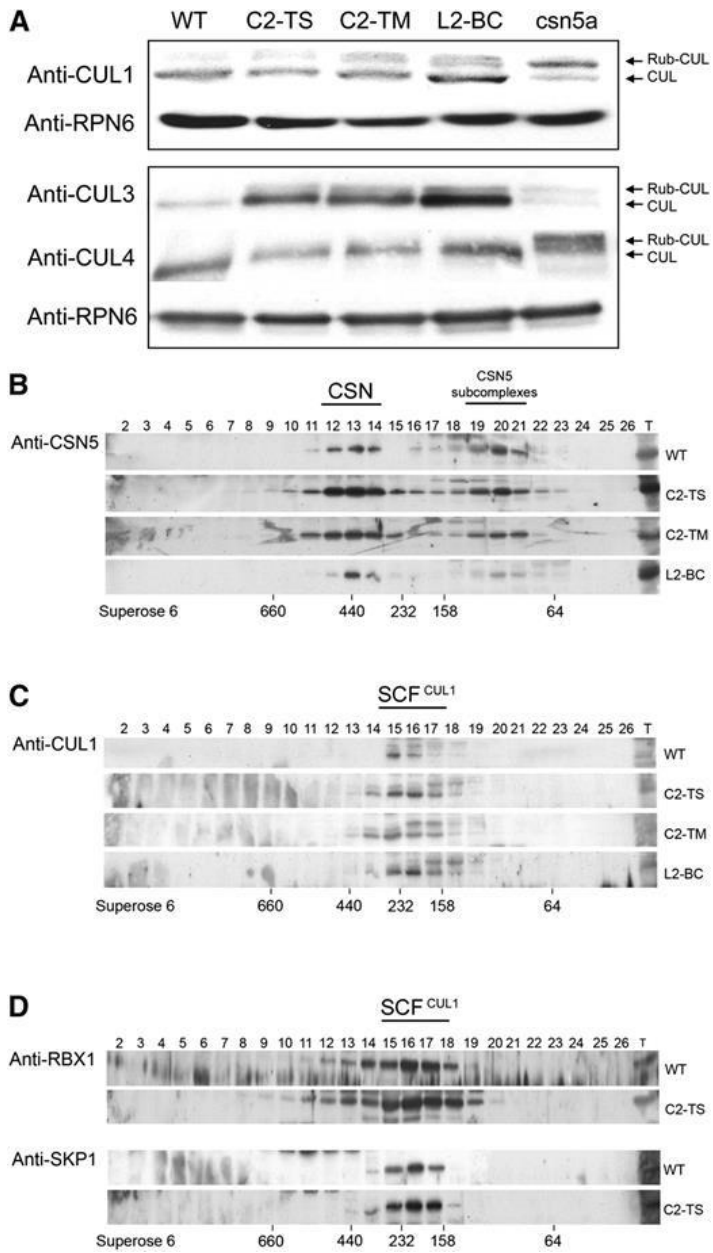
1295

1296

1297

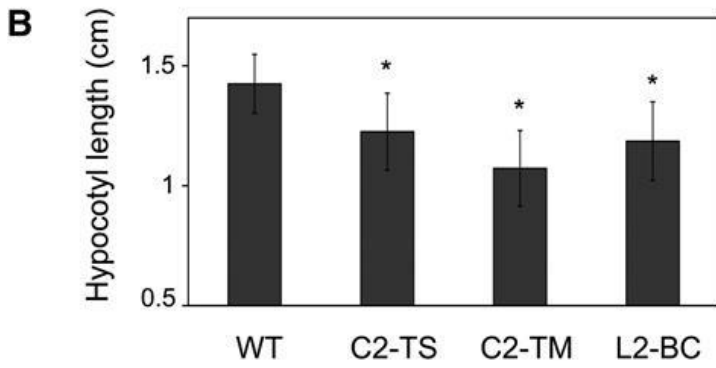
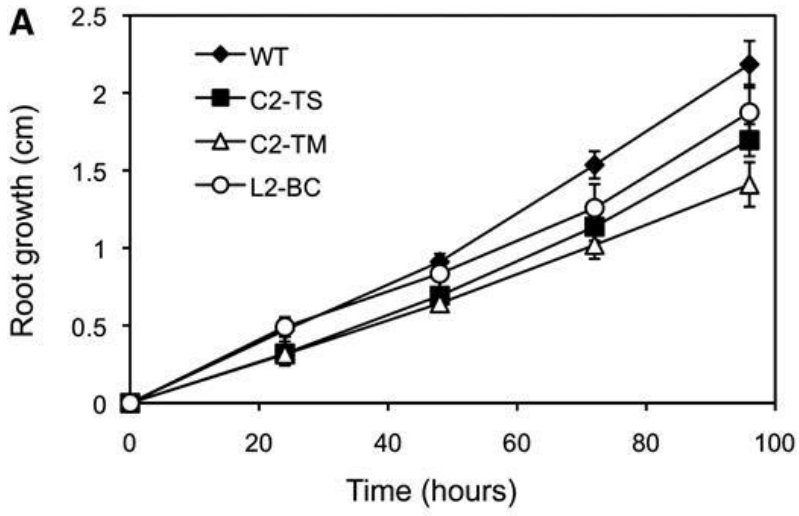
1298

1299 Fig. 2



1300

1301 Fig. 3



1302

1303

1304

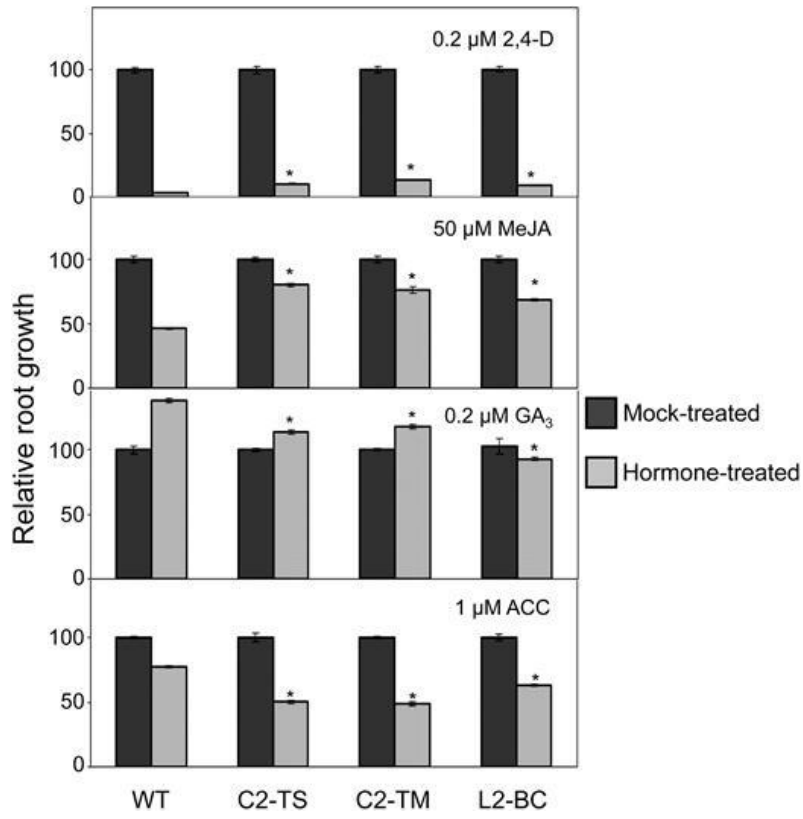
1305

1306

1307

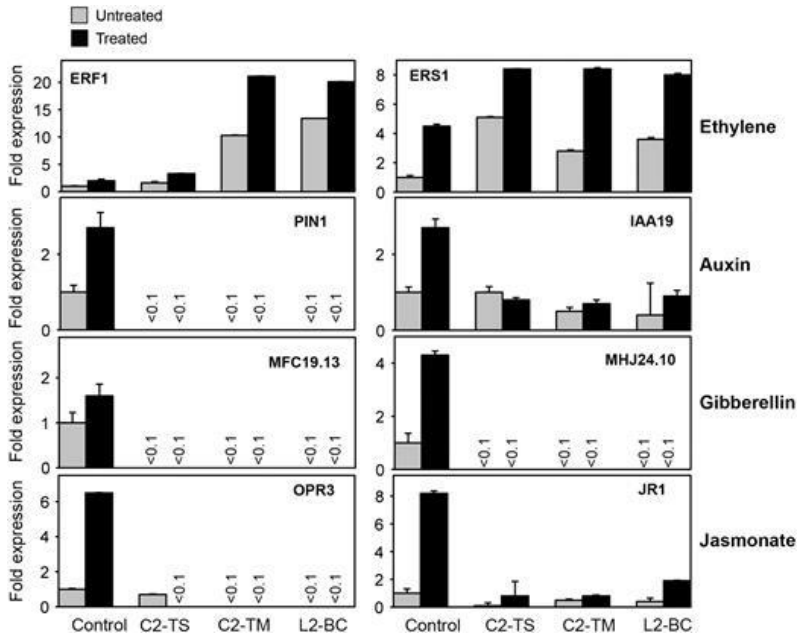
1308

1309 Fig. 4



1310
1311
1312
1313
1314
1315
1316
1317
1318

1319 Fig.5



1320

1321

1322

1323

1324

1325

1326

1327

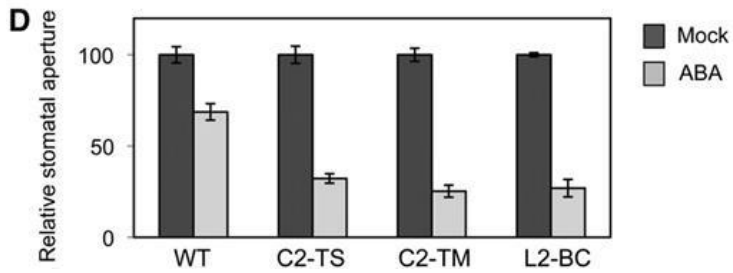
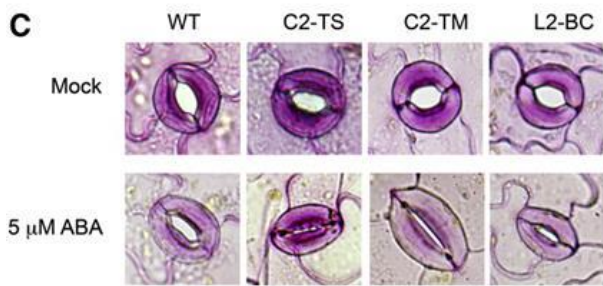
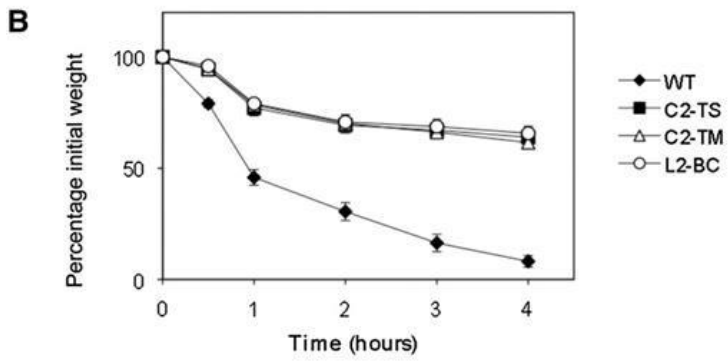
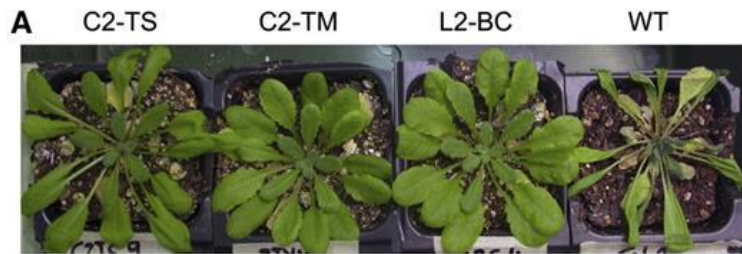
1328

1329

1330

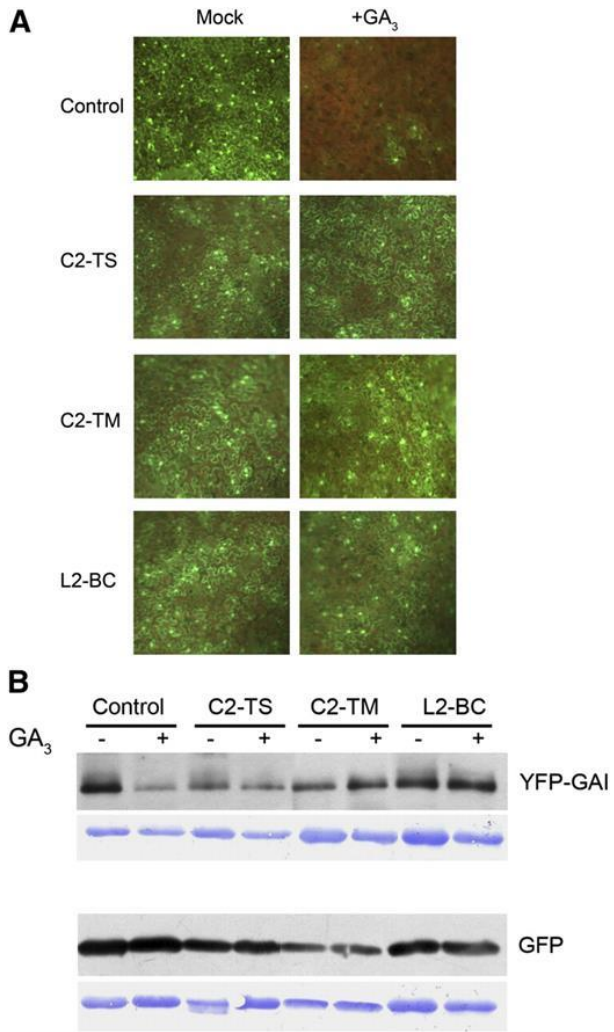
1331

1332 Fig. 6



1333

1334 Fig. 7



1335

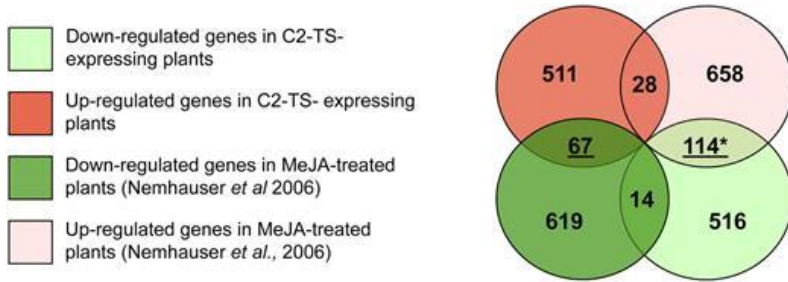
1336

1337

1338

1339

1340 Fig. 8



1342 Fig. 9

